



RESUMEN FINAL PROYECTO INVESTIGACIÓN

EXPEDIENTE: 2019I039

TÍTULO DEL PROYECTO: Uso de exosomas de células madre como terapia en la neuroinflamación inducida por el consumo de alcohol durante la adolescencia y búsqueda de biomarcadores y diferencias de género

INVESTIGADOR PRINCIPAL: María Pascual Mora

EQUIPO DE INVESTIGACIÓN (nombre y apellidos del resto del equipo de investigación):

Consuelo

Guerrí Sirera

Marta

Rodríguez Arias

Sandra

Montagud Romero

ENTIDAD BENEFICIARIA Y CENTRO DE INVESTIGACIÓN:

Universidad de Valencia, Facultad de Medicina

RESUMEN (1) (2):

Nuestro interés en los últimos años se ha centrado en la búsqueda de terapias para paliar la neuroinflamación producida por el consumo de alcohol durante la adolescencia, y las consecuencias conductuales que se derivan de dicho consumo. El cerebro adolescente está sometido a cambios estructurales y funcionales que hacen que éste sea un órgano especialmente sensible o vulnerable a muchos estímulos, entre los que se encuentran el alcohol.

Hay que destacar que los últimos estudios apuntan al papel terapéutico de unas vesículas extracelulares (VEs), liberadas por las células madre mesenquimales debido a que poseen un alto contenido en biomoléculas funcionales. Por tanto, uno de los objetivos de este proyecto era estudiar el papel de las VEs procedentes de células madre mesenquimales como terapia en la neuroinflamación producida por el consumo de alcohol en atracón en animales adolescentes, analizando parámetros asociados con la respuesta neuroinflamatoria, cambios estructurales en la mielina y sinapsis y alteraciones cognitivas. Además, puesto que los lípidos son un componente importante en los procesos de formación, liberación e interacción celular de los exosomas, es por ello que se analizaron diferencias de género y la implicación del receptor TLR4 en los efectos del alcohol sobre el contenido lipídico de las VEs procedentes de plasma de chicas y chicos adolescentes, y de animales macho y hembra, todo ello para la búsqueda de un biomarcador plasmático.



Nuestros resultados han demostrado que las VEs procedentes de células madre mesenquimales del tejido adiposo son capaces de disminuir la expresión de genes neuroinflamatorios (p. ej., COX-2, iNOS, MIP-1 α , NF- κ B, CX3CL1 y MCP-1) inducidos por el etanol en la corteza prefrontal de ratones adolescentes. En particular, estas VEs también son capaces de restaurar tanto las alteraciones sinápticas y en la mielina, como los trastornos en los procesos de memoria y aprendizaje, inducidos por el tratamiento de etanol en atracón.

Además, nuestros resultados también han demostrado que la intoxicación aguda por etanol indujo un mayor enriquecimiento de distintas especies de lípidos en las VEs procedentes de plasma de mujeres adolescentes que en hombres. Se observó un mayor contenido de las clases de lípidos PA, LPC, FA insaturados y FAHFA en las mujeres, mientras que los hombres mostraron un enriquecimiento en PI. Estas clases de lípidos participan en la formación, liberación y absorción de VEs y en la activación de la respuesta inmune. Además, también se observaron cambios en la composición lipídica en las VEs en ratones WT y TLR4-KO tratados con etanol (p. ej., enriquecimiento de glicerofosfoinositoles en machos WT tratados con etanol). Todos los datos y resultados generados en este estudio se publicaron de forma abierta en una plataforma web (<http://bioinfo.cipf.es/sal>).

ABSTRACT (English):

Our interest in recent years has focused on the search for therapies to alleviate the neuroinflammation caused by binge alcohol drinking during adolescence, and the behavioral consequences derived by this consumption. The adolescent brain suffers structural and functional changes that make it an organ that is especially sensitive to many stimuli, including alcohol.

It should be noted that the latest studies point to the therapeutic role of the extracellular vesicles (EVs), released by mesenchymal stem cells, because they have a high content of functional biomolecules. Therefore, one of the objectives of this project was to study the role of EVs derived by mesenchymal stem cells as a therapy in the neuroinflammation induced by binge alcohol drinking in adolescent animals, analyzing parameters associated with the neuroinflammatory immune response, structural changes in myelin and synapses and cognitive alterations. Furthermore, since lipids are an important component in the processes of formation, release and cellular interaction of EVs, gender differences and the involvement of the TLR4 receptor in the effects of alcohol on the lipid content of the EVs were also analyzed. EVs were isolated from plasma of human adolescent females and males, and from male and female animals, to search for a plasma biomarker.

Our results have shown that EVs derived by mesenchymal stem cells from adipose tissue are capable of decreasing the expression of neuroinflammatory genes (e.g., COX-2, iNOS, MIP-1 α , NF- κ B, CX3CL1 and MCP-1) induced by ethanol in the prefrontal cortex of adolescent mice. In particular, these EVs are also able to restore both synaptic and myelin alterations, as well as memory and learning dysfunction induced by ethanol treatment.

Furthermore, our results have also demonstrated that acute ethanol intoxication induced a greater enrichment of different lipid species in plasma EVs in adolescent females than in males. A higher content of the lipid classes PA, LPC, unsaturated FA and FAHFA was observed in women, while men showed an enrichment in PI. These lipid classes participate in the formation, release and absorption of EVs and in the activation of the immune response. Furthermore, changes in lipid composition were also observed in EVs in ethanol-treated WT and TLR4-KO mice (e.g., enrichment of glycerophosphoinositols in ethanol-treated WT males). All data and results generated have been made openly available on a web-based platform (<http://bioinfo.cipf.es/sal>).

PALABRAS CLAVE (3):

Alcohol, tratamiento, vesículas extracelulares, adolescencia, lipidómica, datos en abierto.



KEY WORDS (English):

Alcohol, treatment, extracellular vesicles, adolescence, lipidomics, open data.

JUSTIFICACIÓN DEL PROYECTO Y OBJETIVOS:

1) Estudiar el papel de las VEs procedentes de células madre mesenquimales de tejido adiposo como terapia en la neuroinflamación producida por el alcohol.

2) Evaluar si la terapia con VEs procedentes de células madre mesenquimales de tejido adiposo es capaz de paliar las alteraciones cognitivas y comportamentales producidas por el consumo de alcohol durante la adolescencia.

3) Estudiar diferencias de género y búsqueda de un biomarcador en los efectos del alcohol sobre la alteración en el contenido lipídico de las VEs procedentes de plasma de chicas y chicos adolescentes y de plasma de animales silvestres (WT) y deficientes en la proteína TLR4 (TLR4-KO) macho y hembra.

METODOLOGÍA Y DESARROLLO DEL PROYECTO. ANALISIS ESTADÍSTICO:

Por un lado, se administraron las VEs procedentes de células madre mesenquimales obtenidas del tejido adiposo en la vena de la cola (50 µg/dosis, una dosis semanal) a ratones adolescentes hembra WT tratados de forma intermitente con etanol (3,0 g/kg) durante dos semanas. Al finalizar el tratamiento, se obtuvo la corteza prefrontal para el análisis de la expresión de genes y estudio de la mielina y sinapsis. Otros animales se destinaron a llevar a cabo pruebas de conducta, como el reconocimiento del objeto nuevo, la evitación pasiva y el laberinto Hebb-Williams. Los resultados se mostraron como la media ± SEM. Todos los parámetros estadísticos empleados se calcularon con el programa SPSS v28. Se utilizó la prueba de Shapiro-Wilk para probar la normalidad de la distribución de los datos. Se utilizó ANOVA de una vía o de dos vías como pruebas paramétricas y como alternativas no paramétricas la prueba U de Mann-Whitney o la prueba de Kruskal-Wallis. Se consideraron estadísticamente significativos valores de $p \leq 0,05$.

Por otro lado, también se utilizaron las VEs procedentes de plasma de mujeres y hombres adolescentes y de ratones adolescentes de tipo salvaje (WT) y con deficiencia en el receptor TLR4 (TLR4-KO). Se realizaron análisis exploratorios y de pre-procesamiento después de la extracción de los lípidos de las VEs y de la adquisición de datos mediante espectrometría de masas. Se utilizaron comparaciones entre individuos machos y hembras intoxicados con etanol y control y ratones machos y hembras WT y TLR4-KO tratados y no con etanol, para analizar la abundancia diferencial de lípidos. Se llevaron a cabo una anotación de lípidos en sus correspondientes clases y un análisis de enriquecimiento del conjunto de lípidos para evaluar las funciones biológicas. Los niveles de abundancia de lípidos entre grupos se compararon utilizando el paquete limma R. Los valores de p se ajustaron utilizando el procedimiento de Benjamini y Hochberg, y los lípidos significativos se consideraron con un valor de p ajustado por el procedimiento de Benjamini y Hochberg de $\leq 0,05$.

PRINCIPALES RESULTADOS:

Nuestros resultados han demostrado que las VEs procedentes de células madre mesenquimales del tejido adiposo son capaces de disminuir la expresión de genes neuroinflamatorios (p. ej., COX-2, iNOS, MIP-1 α , NF- κ B, CX3CL1 y MCP-1) inducidos por el etanol en la corteza prefrontal de ratones adolescentes. En particular, estas VEs también son capaces de restaurar tanto las alteraciones sinápticas y en la mielina, como los trastornos en los procesos de memoria y aprendizaje, inducidos por el tratamiento de etanol en atracán.

Además, nuestros resultados también han demostrado que la intoxicación aguda por etanol indujo un mayor enriquecimiento de distintas especies de lípidos en las VEs procedentes de plasma de mujeres adolescentes que en hombres. Se observó un mayor contenido de las clases de lípidos PA, LPC, FA insaturados y FAHFA en las mujeres, mientras que los hombres mostraron un



enriquecimiento en PI. Estas clases de lípidos participan en la formación, liberación y absorción de VEs y en la activación de la respuesta inmune. Además, también se observaron cambios en la composición lipídica en las VEs en ratones WT y TLR4-KO tratados con etanol (p. ej., enriquecimiento de glicerofosfinosítoles en machos WT tratados con etanol). Todos los datos y resultados generados en este estudio se publicaron de forma abierta en una plataforma web (<http://bioinfo.cipf.es/sal>).

DISCUSIÓN:

Nuestros estudios previos demostraron el papel de las VEs como amplificadores de la respuesta neuroinflamatoria a través del receptor TLR4 inducida por el tratamiento de etanol en células astrogiales en cultivo y en experimentos *in vivo* en tejido cerebral. Sin embargo, diferentes estudios recientes también ponían de manifiesto el potencial papel de las VEs como agentes terapéuticos de diferentes enfermedades, como los trastornos neurodegenerativos y el daño cerebral. Estudios experimentales han evidenciado las propiedades antiinflamatorias y antioxidantes de las VEs procedentes de células madre mesenquimales en la activación de la respuesta inmune a través del TLR4 inducida por su ligando específico, el lipopolisacárido. De acuerdo con estos hallazgos, estos estudios demuestran que las VEs procedentes de células madre mesenquimales pueden prevenir el aumento de la expresión de genes inflamatorios (p. ej., iNOS, MIP-1 α , NF- κ B y CX3CL1) inducidos por el tratamiento de etanol en forma de atracción en adolescentes.

Los presentes resultados muestran que la inyección intravenosa de VEs procedentes de células madre mesenquimales en ratones adolescentes tratados con etanol en altas cantidades es capaz de reducir tanto las alteraciones en la materia blanca (p. ej., formas irregulares de las fibras de mielina, división interlamina de las vainas de mielina), como los cambios ultraestructurales en las sinapsis, como una reducción tanto del espesor postsináptico como del número de vesículas sinápticas. En línea con nuestros resultados, un estudio en monos rhesus con lesión cortical demostró que la administración de VEs procedentes de células madre mesenquimales puede promover acciones terapéuticas a través de la recuperación de la estructura de las neuronas piramidales premotoras y la función dendrítica. Por lo tanto, estos efectos neuroprotectores de las VEs procedentes de células madre mesenquimales se pueden atribuir no solo a sus propiedades antiinflamatorias, sino también a la regulación en la expresión de genes relacionados con la mielina en el daño cerebral.

Datos recientes demuestran la participación de las VEs procedentes de células madre mesenquimales en la protección de los déficits de la memoria en el espacio-temporal y los trastornos del aprendizaje inducidos por LPS, según lo evaluado mediante las pruebas del reconocimiento de objeto nuevo y el laberinto de Barnes. La reparación de la función cognitiva mediante el uso de VEs procedentes de células madre mesenquimales también se ha demostrado en modelos animales de enfermedades neurodegenerativas, como la enfermedad de Alzheimer, lesión cerebral, enfermedad de Parkinson y esquizofrenia, entre otras. En particular, el presente estudio demuestra que las VEs procedentes de células madre mesenquimales mejoran la disfunción de la memoria en el espacio-temporal inducida por el etanol, así como los déficits de la memoria y del aprendizaje, según lo evaluado por las pruebas del reconocimiento de objeto nuevo, la evitación pasiva y el laberinto de Hebb-Williams. De hecho, hemos demostrado que la administración de VEs procedentes de células madre mesenquimales es capaz de normalizar la disfunción para reconocer el objeto nuevo, un tiempo de latencia más corto durante la prueba de la evitación pasiva y el tiempo para completar los laberintos de Hebb-Williams en los ratones adolescentes tratados con etanol.

Nuestros resultados también ponen de manifiesto la existencia de diferencias de sexo, entre adolescentes mujeres y hombres en el perfil lipídico de las VEs tras un consumo excesivo de alcohol. Dada la gran vulnerabilidad de las mujeres a los efectos del alcohol, este trabajo sugiere diferencias de sexo en los lípidos de las VEs que nos pueden ayudar a comprender mejor los mecanismos implicados en el consumo de alcohol y también nos pueden proporcionar adecuados biomarcadores plasmáticos (p. ej., TG 16:0_18:1_20:3 y Cer_NDS d39:1 en hembras y machos



humanos). Este estudio adopta un enfoque novedoso para evaluar las diferencias de sexo en el efecto del etanol en el perfil lipídico a través de una estrategia bioinformática integral.

Sin embargo, el estudio del perfil lipídico de las VEs de plasma presentó diversas limitaciones. Por ejemplo, el uso de la tecnología de la lipidómica en este estudio presentó un desafío con respecto al diseño y aplicación de la estrategia bioinformática que se debía de abordar, en cuanto a: 1) la falta de estandarización en la nomenclatura de lípidos y su integración en el software de análisis, 2) la falta de metodologías de análisis, y 3) la falta de generación de anotaciones funcionales [3]. Además, tampoco podemos descartar que pueda haber diferencias desconocidas entre los sujetos humanos (casos intoxicados con etanol versus controles) que puedan limitar la comparación con respecto a la composición de lípidos entre grupos. A pesar de todo esto, nuestro presente estudio adopta un enfoque novedoso para estudiar las diferencias basadas en el sexo en el efecto del alcohol basándose en el análisis bioinformático de datos lipídicos, y nuestros hallazgos mejoran la comprensión de los efectos del consumo excesivo de alcohol al incluir una perspectiva de género. Todos los datos, resultados y guiones de programación se incluyeron en recursos abiertos (plataforma web y repositorio Zenodo) para compartir con la comunidad científica.

APLICABILIDAD E IMPACTO SOCIO-SANITARIO DEL PROYECTO:

Puesto que en los últimos años se ha investigado mucho sobre la función de las VEs, y actualmente está en el punto de mira el uso de estas microvesículas en terapia, estos resultados confirman el papel de las VEs procedentes de células madre mesenquimales como posible terapia para bloquear los efectos neurotóxicos y conductuales del abuso del alcohol durante la adolescencia. Al mismo tiempo, también se está trabajando para obtener un buen biomarcador plasmático que nos pudiera dar información sobre el daño en cerebro producido por la activación de la respuesta neuroinflamatoria tras el consumo de alcohol durante la adolescencia. Se conoce el uso de los microARNs procedentes de las VEs en su uso como biomarcadores, pero poco se conoce hasta el momento de las especies lipídicas de estas microvesículas. Por tanto, la utilización de muestras procedentes de plasma de humano y de ratón, nos ha ayudado a obtener posibles especies lipídicas que pueden ser usadas como biomarcadores plasmáticos. De esta forma, el estudio y búsqueda de lípidos de las VEs utilizados como posibles biomarcadores es otra estrategia que se ha tenido en cuenta en el presente proyecto que nos puede ayudar a determinar el diagnóstico y seguimiento del daño cerebral producido por el consumo de alcohol durante la adolescencia.

SÍNTESIS DE LOS ASPECTOS MÁS RELEVANTES QUE APORTA EL ESTUDIO:

Nuestros resultados ponen de manifiesto el papel neuroprotector de las VEs procedentes de células madre mesenquimales no sólo en la respuesta inmune neuroinflamatoria, sino también en las alteraciones de la mielina y sinapsis y en la disfunción cognitiva inducida por el tratamiento de etanol en atracción durante la adolescencia. Por tanto, estos hallazgos evidencian el potencial terapéutico de las VEs procedentes de células madre mesenquimales y pueden proporcionar una nueva herramienta para tratar la neuroinflamación asociada con el consumo de alcohol y otras enfermedades neurodegenerativas.

Nuestros resultados también sugieren que el consumo excesivo de etanol en individuos adolescentes conduce a un mayor contenido de especies de lípidos en las VEs de plasma de mujeres, que se asocian con la biogénesis de las VEs y con la propagación de la respuesta neuroinflamatorias que en los hombres. Además, existen mayores diferencias en la abundancia de lípidos entre sexos en ratones WT en comparación con ratones TLR4-KO. Por último, estos resultados también respaldan el potencial uso de los lípidos en las VEs como biomarcadores de la neuroinflamación inducida por el consumo de etanol durante la adolescencia.



ENLACES O REFERENCIAS PARA AMPLIAR INFORMACIÓN ACERCA DEL PROYECTO (en su caso):

<http://bioinfo.cipf.es/sal>

PUBLICACIONES CIENTÍFICAS GENERADAS (4) (SI NO LO HA HECHO, LE ROGAMOS ENVÍE JUNTO CON ESTA FICHA COPIA DE CADA UNO DE LOS TRABAJOS PUBLICADOS)

- C. Perpiñá-Clérigues, S. Mellado, J.F. Català-Senent, F. Ibáñez, P. Costa, M. Marcos, C. Guerri, M. Pascual. Lipidomics landscape of circulating extracellular vesicles isolated from adolescents exposed to ethanol intoxication: A sex difference study. *Biol. Sex Differ.* 2023;14(1): 22. DOI: 10.1186/s13293-023-00502-1

- S. Mellado, C.M. Cuesta, P. S. Montagud-Romero, M. Rodríguez-Arias, V. Moreno-Manzano, C. Guerri, M. Pascual. Therapeutic role of mesenchymal stem cell-derived extracellular vesicles in neuroinflammation and cognitive dysfunctions induced by binge-like ethanol treatment in adolescent mice. *CNS Neurosci. Ther.* 2023. DOI: 10.1111/cns.14326

Otras publicaciones en las que se ha incluido al PNSD:

- F. Ibáñez, J. Montesinos, J.R. Ureña-Peralta, C. Guerri*, M. Pascual*. TLR4 participates in the transmission of ethanol-induced neuroinflammation via astrocyte-derived extracellular vesicles. *J. Neuroinflammation* 2019;16(1):136. DOI: 10.1186/s12974-019-1529-x.

- M. Pascual*, F. Ibáñez, C. Guerri*. Exosomes as mediators of neuron-glia communication in neuroinflammation. *Neural Regen. Res.* 2020;5(5):796-801.

- M. Pascual, J.R. Ureña-Peralta, C. Guerri. The regulatory role of miRNAs in ethanol-induced TLR4 activation and neuroinflammation. *Curr. Pathobiol. Rep.* 2020;37:45.

- F. Ibáñez, J.R. Ureña-Peralta, P. Costa-Alba, J.L. Torres, F.J. Laso, M. Marcos, C. Guerri, M. Pascual. Circulating microRNAs in extracellular vesicles as potential biomarkers of alcohol-induced neuroinflammation in adolescence: Gender differences. *Int. J. Mol. Sci.* 2020;21:6730.

- M. Pascual, R. López-Hidalgo, S. Montagud-Romero, J.R. Ureña-Peralta, M. Rodríguez-Arias, C. Guerri. Role of mTOR-regulated autophagy in spine pruning defects and memory impairments induced by binge-like ethanol treatment in adolescent mice. *Brain Pathol.* 2021;31:174-188.

- C.M. Cuesta, C. Guerri, J. Ureña, M. Pascual. Role of microbiota-derived extracellular vesicles in gut-brain communication. *Int. J. Mol. Sci.* 2021;22:4235.

- F. Ibáñez, J. Montesinos*, E. Area-Gomez, C. Guerri, M. Pascual*. Ethanol induces extracellular vesicle secretion by altering lipid metabolism through the mitochondria-associated ER membranes and sphingomyelinases. *Int. J. Mol. Sci.* 2021;22:8438.

- M. Pascual, M. Calvo-Rodríguez, L. Núñez, C. Villalobos, J. Ureña, C. Guerri. Toll-like receptors in neuroinflammation, neurodegeneration, and alcohol-induced brain damage. *IUBMB Life* 2021; 73(7): 900-915.

PRESENTACIÓN DE RESULTADOS (CONGRESOS, JORNADAS Y ACTIVIDADES DE DISEMINACIÓN CIENTÍFICA Y TÉCNICA):

- Congreso LASBRA (Latin American Society for Biomedical Research on Alcoholism). Virtual, Diciembre, 2020.

M. Pascual. Exosomes as carriers and biomarkers of the ethanol induced neuroinflammation in adolescents with binge drinking.



- Congreso XV European Meeting on Glial Cells in Health and Disease. Marsella-Virtual, Julio, 2021.
C. Guerri, F. Ibáñez, M. Pascual. Extracellular vesicles secreted by ethanol-treated astrocytes participates in glial-neuron communication spreading the neuroinflammation via TLR4. Simposio S29-01.

- Congreso RSA. San Antonio-Virtual, Junio, 2021.
C. Guerri, F. Ibáñez, J. Ureña-Peralta, M. Pascual. Astrocytes-derived exosomes act as cellular transmitters contributing to spread the neuroinflammation induced by ethanol. Simposio.

- Congreso ESBRA. Timisoara, Octubre, 2021.
M. Pascual, F. Ibáñez, C Guerri. Role of exosomes as biomarkers of the neuroinflammation induced by adolescent binge drinking. Revista de la ESBRA, 2021; S5 (20).
Comunicación oral: M. Pascual

- Congreso ESBRA. Timisoara, Octubre, 2021.
M. Pascual, C. Perpiñá-Clérigues, J.F. Català-Senent, F. Ibáñez, C. Guerri, F. García-García. Sex differences in the lipidomic profile of extracellular vesicles of adolescents exposed to alcohol intoxication. Revista de la ESBRA, 2021; Poster 103.

- Congreso ISBRA/ESBRA. Cracovia, Septiembre, 2022.
S. Mellado, C.M. Cuesta, V. Moreno-Manzano, C. Guerri, M. Pascual. Role of extracellular vesicles derived by mesenchymal stem cells in the neuroinflammation induced by intermittent ethanol treatment in adolescence.
Comunicación oral: M. Pascual

- 21st European Conference on Computational Biology. Sitges, Septiembre, 2022.
C. Perpiñá-Clérigues, J.F. Català-Senent, S. Mellado, C. Guerri, M. Pascual, F. García-García. Ethanol-induced sex-based differences in the extracellular vesicles lipidome. Libro de Abstracts, 2022;422.

- Congreso de Alcoholism and Stress. Volterra, Mayo, 2023.
S. Mellado, C.M. Cuesta, C. Guerri, M. Pascual. Adipose-derived stem cell extracellular vesicles ameliorate the neuroinflammation induced by binge drinking in adolescence. Alcohol Journal (Elsevier), 2023;109 (S11). Comunicación oral: M. Pascual

PATENTES Y MODELOS DE UTILIDAD (en su caso) :

BIBLIOGRAFÍA (4):

COFINANCIACIÓN (APARTE DE LA DELGACIÓN DEL GOBIERNO PARA EL PLAN NACIONAL SOBRE DROGAS), en su caso:

AGRADECIMIENTOS:

Se agradece al Centro de Investigación Príncipe Felipe (CIPF) por proporcionarnos acceso al clúster para el almacenamiento de datos del estudio lipidómico, que está cofinanciado por los Fondos Europeos de Desarrollo Regional (FEDER) en la Comunidad Valenciana 2014-2020. Los autores también agradecen a la Unidad de Genómica y Proteómica de la Universidad de Alicante, al Servicio de Microscopía Electrónica del Centro de Investigación Príncipe Felipe.



CONTACTO (dirección de correo electrónico para consultas al equipo de investigación):

maria.pascual@uv.es

NOTAS:

(1): Este resumen está dirigido a dar a conocer los aspectos sustanciales de los proyectos financiados por la Delegación del Gobierno para el Plan Nacional sobre Drogas tanto a la población general como a profesionales, a través de su publicación en la página web del Ministerio de Sanidad. Procure ser conciso en las exposiciones. Incluya las gráficas y tablas que considere oportunas. En el caso de precisar otro tipo de información (audiovisuales, archivos de datos, etc.), consulte con el órgano instructor para valorar procedimiento de difusión.

(2): Máximo 500 palabras.

(3): Utilice como fuente el Medical Subjects Headings, MeSH, del Index Medicus.

(4) Se recomienda seguir los Requisitos de Uniformidad del Comité Internacional de Directores de Revistas Médicas conforme a las normas de la US National Library of Medicine (<https://www.ncbi.nlm.nih.gov/books/NBK7250/>)

Therapeutic role of mesenchymal stem cell-derived extracellular vesicles in neuroinflammation and cognitive dysfunctions induced by binge-like ethanol treatment in adolescent mice

Susana Mellado¹ | Carlos M. Cuesta¹ | Sandra Montagud² | Marta Rodríguez-Arias² | Victoria Moreno-Manzano³ | Consuelo Guerri⁴ | María Pascual¹ 

¹Department of Physiology, School of Medicine and Dentistry, University of Valencia, Valencia, Spain

²Department of Psychobiology, Facultad de Psicología, Universitat de Valencia, Valencia, Spain

³Neuronal and Tissue Regeneration Laboratory, Príncipe Felipe Research Center, Valencia, Spain

⁴Príncipe Felipe Research Center, Valencia, Spain

Correspondence

María Pascual, Department of Physiology, School of Medicine and Dentistry, University of Valencia, Avda. Blasco Ibáñez, 15, 46010 Valencia, Spain.
Email: maria.pascual@uv.es

Funding information

Generalitat Valenciana, Grant/Award Number: CIAICO/2021/203 and CIPROM/2021/080; the Carlos III Institute, Grant/Award Number: RD16/0017/0004; the Primary Addiction Care Research Network, Grant/Award Number: RD21/0009/0005; the Spanish Ministry of Health, Grant/Award Number: 2018-I003 and 2019-I039

Abstract

Background: Extracellular vesicles (EVs) are heterogeneous membrane vesicles secreted by cells in extracellular spaces that play an important role in intercellular communication under both normal and pathological conditions. Mesenchymal stem cells (MSC) are anti-inflammatory and immunoregulatory cells capable of secreting EVs, which are considered promising molecules for treating immune, inflammatory, and degenerative diseases. Our previous studies demonstrate that, by activating innate immune receptors TLR4 (Toll-like receptor 4), binge-like ethanol exposure in adolescence causes neuroinflammation and neural damage.

Aims: To evaluate whether the intravenous administration of MSC-derived EVs is capable of reducing neuroinflammation, myelin and synaptic alterations, and the cognitive dysfunction induced by binge-like ethanol treatment in adolescent mice.

Materials & Methods: MSC-derived EVs obtained from adipose tissue were administered in the tail vein (50 microg/dose, one weekly dose) to female WT adolescent mice treated intermittently with ethanol (3.0 g/kg) during two weeks.

Results: MSC-derived EVs from adipose tissue ameliorate ethanol-induced up-regulation of inflammatory genes (e.g., COX-2, iNOS, MIP-1 α , NF- κ B, CX3CL1, and MCP-1) in the prefrontal cortex of adolescent mice. Notably, MSC-derived EVs also restore the myelin and synaptic derangements, and the memory and learning impairments, induced by ethanol treatment. Using cortical astroglial cells in culture, our results further confirm that MSC-derived EVs decrease inflammatory genes in ethanol-treated astroglial cells. This, in turn, confirms *in vivo* findings.

Conclusion: Taken together, these results provide the first evidence for the therapeutic potential of the MSC-derived EVs in the neuroimmune response and cognitive dysfunction induced by binge alcohol drinking in adolescence.

This is an open access article under the terms of the [Creative Commons Attribution](https://creativecommons.org/licenses/by/4.0/) License, which permits use, distribution and reproduction in any medium, provided the original work is properly cited.

© 2023 The Authors. *CNS Neuroscience & Therapeutics* published by John Wiley & Sons Ltd.

KEYWORDS

adolescence, binge-like ethanol treatment, cognitive dysfunction, extracellular vesicles, mesenchymal stem cells, neuroinflammation

1 | INTRODUCTION

Mesenchymal stem cells (MSC) are adult stem cells capable of stimulating the maintenance, growth, and survival of other cells.¹ Their therapeutic potential seems to be mediated by the paracrine factors contained in microvesicles.² Indeed the extracellular vesicles (EVs) that derive from MSC (MSC-EVs) display a different genetic cargo and protein content, which play a significant role in biological processes, including regulation of inflammation, apoptosis, angiogenesis, adipogenesis, blood coagulation, and extracellular matrix remodeling.³ However, MSC-EVs have emerged as therapeutic agents to reduce tissue injury and enhance tissue repair in cerebral injury, lung injury, myocardial injury, and kidney injury cases.^{4,5}

Extracellular vesicles are microvesicles that originate from multivesicular bodies and can be isolated from diverse body fluids and multiple cell cultures supernatants.⁶ The content of EVs is complex in nature and includes several types of proteins, RNAs, miRNAs, enzymes, and lipids, which act as messengers during cell-to-cell communication in multiple physiological and pathological processes.⁷⁻⁹ Analyses of MSC-EVs have demonstrated that their content is enriched in miRNAs and proteins.³ In the central nervous system, neuron- and astrocyte-derived EVs play critical roles in several processes, such as promoting neurite outgrowth, synaptic plasticity, neuronal survival, and neuroprotection,⁷ MSC-EVs can recover the neuronal and astroglial damage induced by several injuries.¹⁰

The adolescent brain shows important changes in its structure and function,¹¹ including synaptic plasticity and neural connectivity, which especially occur in the prefrontal cortex (PFC) and other subcortical areas.^{12,13} These extensive developing changes in brain maturation might explain the adolescent brain's vulnerability to the deleterious effects of ethanol.^{14,15} Our previous studies have demonstrated that by activating innate immune receptors TLR4 (Toll-like receptor 4) in glial cells, binge-like ethanol exposure in adolescence leads to the release of cytokines and chemokines, and causes neuroinflammation and neural damage.^{16,17} Activation of the TLR4 response has also been demonstrated in myelin and synaptic alterations, as well as cognitive and behavioral impairments, induced by binge drinking in adolescent mice.¹⁸ This scenario suggests the involvement of the neuroinflammatory immune response in behavioral deficits. Indeed human studies have shown that the one brain region most affected by ethanol drinking in adolescence is the PFC, a region associated with cognitive control and executive function.¹⁹ Likewise, myelin dysfunctions have been related to attention and spatial working memory deficits in human adolescents with heavy alcohol abuse.²⁰

In agreement with the therapeutic beneficial effects of MSC-EVs to treat neurological and neurodegenerative diseases,²¹ the

present study provides evidence that the intravenous administration of MSC-EVs from adipose tissue ameliorates neuroinflammation, as well as myelin and synaptic alterations, which lead to the cognitive impairments induced by binge-like ethanol treatment in adolescent mice.

2 | MATERIALS AND METHODS

2.1 | MSC isolation, culture, and isolation of MSC-EVs

Human adipose tissue was obtained from surplus fat tissue during knee prosthesis operation performed on four patients under sterile conditions. Human samples were anonymized. The experimental procedure was previously evaluated and accepted by the Regional Ethics Committee for Clinical Research with Medicines and Health Products following Code of Practice 2014/01. As the exclusion criteria, no samples were collected from patients with a history of cancer or infectious diseases at the time of (viral or bacterial) surgery. All the human patients voluntarily signed an informed consent document to use the adipose samples. Cells were expanded and grown in the growth medium [GM: High glucose DMEM basal medium supplemented with 20% FBS (previously centrifuged at 100000×g for 1 h for EV depletion and then filtered by a 0.2 μm filter), 100 units/mL penicillin, 100 μg/mL streptomycin and 2 mM L-glutamine in]. MSC have been characterized and previously described.^{22,23} Subconfluent cells were incubated in GM for 48 h. Then, media were collected and cleared from detached cells and cell fragments by centrifugation at 300×g for 10 min, and by the supernatant at 2000×g for 10 min, respectively. Subsequently, apoptotic bodies and other cellular debris were pelleted by centrifuging the resulting supernatant at 10000×g for 30 min. EVs were then pelleted from the previous resulting supernatant at 100000×g for 1 h. The EVs pellet was washed with PBS and centrifuged at 100000×g for 1 h. EVs were finally suspended in 100 mL PBS and stored at -80°C.

2.2 | Animals and treatments

Ninety-two female C57BL/6 WT (wild-type) mice (Harlan Ibérica) were used. Mice were housed (3-4 animals/cage) and maintained on a water and solid diet ad libitum. Environmental conditions, such as light and dark (12/12 h), temperature (23°C), and humidity (60%), were controlled for all the animals. All the animal experimental procedures were approved by the Ethical Committee of Animal Experimentation of the Principe Felipe Research Center (Valencia, Spain), following the guidelines approved by European Communities

Council Directive (86/609/ECC) and Spanish Royal Decree 53/2013 modified by Spanish Royal Decree 1386/2018.

The intermittent ethanol treatment was initiated early in adolescence or during the prepubescent period on postnatal day (PND) 30.²⁴ Morning doses of either saline or 25% (v/v) ethanol (3 g/kg) in isotonic saline were administered intraperitoneally to 30-day-old mice on two consecutive days with 2-day gaps without injections for 2 weeks (PND30–PND43), as previously described.^{18,25} No signs of peritoneal cavity irritation, pain or distress, or peripheral inflammation induced by intraperitoneal ethanol concentration were noted, which agrees with other studies that have used intraperitoneal ethanol administration.²⁶ After a single ethanol dose, blood alcohol levels peaked at 30 min (~340 mg/dL) and then progressively lowered until 5 h post-injection. Three hours before ethanol administration, animals were also treated with MSC-EVs (50 µg/dose) or saline (sodium chloride, 0.9%) in the tail vein once a week (with the third and seventh ethanol dose). Animals were randomly assigned to four groups according to their treatments: (1) physiological saline or control; (2) physiological saline plus MSC-EVs; (3) ethanol; (4) ethanol plus MSC-EVs. No changes in either animals' body weight or brain weight were observed during the intermittent treatment (Figure S1). Animals were anesthetized 24 h after the last (8th) ethanol or saline administration (PND 44). Brains were removed and transferred to a plate placed on ice. Olfactory bulbs, cerebellum, and pons were removed. Brains were placed with the ventral side facing the plate. We used curved forceps to remove the cortical hemispheres from the rest of the brain. Then the PFC dissection was performed based on visual information and using brain atlas coordinates.^{27,28} PFCs ($n=9-10$ mice/group) were immediately snap-frozen in liquid nitrogen and stored at -80°C until used. In addition, some animals were anesthetized, perfused with paraformaldehyde/glutaraldehyde, and used for the electron microscopy analysis ($n=6$ mice/group). Other animals ($n=10-12$ mice/group) were employed to perform behavioral studies after ethanol treatment on PND 50 in this test daily order: novel object recognition, passive avoidance, and Hebb-Williams maze.

2.3 | Primary culture of astrocytes and treatments

Astroglial cells ($98 \pm 0.5\%$ GFAP-positive cells)²⁹ were obtained from the brain cortices of newborn WT pups (6–8 animals per culture; $n=6$). They were mechanically dissociated and cultured in DMEM (Dulbecco's modified eagle's medium), supplemented with 20% fetal bovine serum (FBS), 100 U/mL penicillin/streptomycin, 2.5 µg/mL fungizone, 2 mM glutamine and 1 g/L glucose, and seeded at 850 cells/mm². On day 7 in vitro, FBS was reduced to 10% and glucose was removed. On day 14 in vitro, cell cultures were 90%–95% confluent and FBS was replaced with bovine serum albumin (BSA, 1 mg/mL) 24 h prior to ethanol (40 mM) stimulation to avoid EVs from being present in FBS. Some plates were incubated with MSC-EVs (2.5 µg) 2 h before the ethanol treatment.

After 24 h of ethanol stimulation, cells were harvested, frozen, and stored at -80°C until further use.

2.4 | Extracellular vesicles characterization by transmission electron microscopy and nanoparticles tracking analysis

The freshly isolated EVs were fixed with 2% paraformaldehyde and prepared as previously described.³⁰ Preparations were examined under a transmission FEI Tecnai G2 Spirit electron microscope (FEI Europe) with a Morada digital camera (Olympus Soft Image Solutions GmbH). In addition, an analysis of the absolute size range and concentration of microvesicles was performed using NanoSight NS300 Malvern (NanoSight Ltd.), as previously described.³⁰

2.5 | Western blot analysis

The Western blot technique was performed in MSC-EVs for their characterization, as described elsewhere.¹⁸ The employed primary antibodies were: anti-CD9, anti-CD63, anti-CD81, and anti-calnexin (Santa Cruz Biotechnology). Membranes were washed, incubated with the corresponding HRP-conjugated secondary antibodies, and developed by the ECL system (ECL Plus; Thermo Scientific). The cell lysate from the astrocyte primary cell culture was used as the negative control for CD9, CD63, and CD81, and as the positive control for calnexin. The full unedited blots are included in the Supplementary Material.

2.6 | RNA isolation, reverse transcription, and quantitative RT-PCR

The frozen PFC samples (10–20 mg) and astroglial cells were used for total RNA extraction. Tissue and cells were disrupted using 1 mL of TRIzol (Sigma-Aldrich), and the total RNA fraction was extracted following the manufacturer's instructions. Total mRNA was reverse-transcribed by the NZY First-Strand cDNA Synthesis Kit (NZYTech, Lda. Genes and Enzymes). Quantitative two-step RT-PCR (real-time reverse transcription) was performed with the Light-Cycler 480 detection System (Roche Diagnostics). Genes were amplified employing the AceQ® qPCR SYBR Green Master Mix (NeoBiotech) following the manufacturer's instructions. The mRNA level of housekeeping gene cyclophilin A was used as an internal control for the normalization of the analyzed genes. All the RT-qPCR runs included non-template controls (NTCs). Experiments were performed in triplicates. Quantification of expression (fold change) from the Cq data was calculated by the $\Delta\Delta\text{Cq}$ method³¹ by the LightCycler 480 relative quantification software (Roche Diagnostics). Details of the nucleotide sequences of the used primers are found in the Supplementary Material (Table S1).

2.7 | Brain tissue preparation and electron microscopy

Mice were anesthetized by an intraperitoneal injection of sodium pentobarbital (60mg/kg) and fentanyl (0.05mg/kg) for analgesia. Animals were then perfused transcardially with 0.9% saline containing heparin, followed immediately by 2% paraformaldehyde and 2.5% glutaraldehyde in 0.1M phosphate buffer, pH7.4, for tissue fixation. The fixed brains were removed, postfixed overnight at 4°C with the same fixative solution, and then stored at 4°C in PBS. After removing the olfactory bulbs, the anterior coronal section, of approximately 1mm was discarded. The following section of approximately 1mm from 2.5 to 1.5mm anterior to Bregma was used to cut PFCs in sections of 200µm on a Leica VT-1000 vibratome (Leica). Sections were post-fixed with 2% osmium, rinsed, dehydrated, and embedded in Durcupan resin (Fluka, Sigma-Aldrich). Semithin sections (1.5µm) were cut with an Ultracut UC-6 (Leica) and stained lightly with 1% toluidine blue. Finally, ultrathin sections (0.08µm) were cut with a diamond knife, stained with lead citrate (Reynolds solution), and examined under a transmission FEI Tecnai G2 Spirit electron microscope (FEI Europe) using a Morada digital camera (Olympus Soft Image Solutions GmbH). Images were analyzed by the ImageJ software (version 1.53a). Synaptic and myelin quantifications were carried out on 4–5 sections per PFC. For each group, 150–175 postsynaptic density thicknesses and 150–175 synaptic cleft width were analyzed. In addition, the number of synaptic vesicles was quantified in 75–100 presynaptic terminals. Damage in the total myelin sheaths was analyzed by measuring the alterations of the total multiple layers of myelin membrane around an axon and was represented as a percentage. Myelin quantification was measured in at least 40–45 axons chosen randomly from each group.

2.8 | Behavioral testing

2.8.1 | Novel object recognition test

Mice performed this test in a black open box (24cm × 24cm × 15cm) using small nontoxic objects: two plastic boxes and a plastic toy. The task procedure is described elsewhere²⁵ and consists of three phases: habituation, training session (T1), and test session (T2). During the habituation session, mice spent 5min exploring the open-field arena where T1 and T2 were performed. During the training session, one mouse was placed in the open-field arena containing two identical sample objects placed in the middle of the testing box for 3min. After a 1-min retention interval, the animal was returned to the open-field arena with two objects during the test session (3min): one object was identical to the sample and the other was novel. Object exploration was defined as the orientation of the animal's snout toward the object within a range of ≤2cm from the object. The recognition index was calculated by measuring the discrimination index $[D.I. = (t_{\text{novel}} - t_{\text{familiar}}) / (t_{\text{novel}} + t_{\text{familiar}}) \times 100\%]$, with "t" taken as the time that each mouse spent exploring an object.

2.8.2 | Passive avoidance test

Step-through inhibitory avoidance apparatus for mice (Ugo Basile) was employed for the passive avoidance test. The cage was made of Perspex sheets and was divided into two compartments (15 × 9.5 × 16.5cm each). The safe compartment was white and illuminated by a light fixture (10W) fastened to the cage lid. The "shock" compartment was dark and made of black Perspex panels. Both compartments were divided by a door that automatically operated by sliding on the floor. The floor was made of 48 stainless steel bars (0.7mm in diameter) placed 8mm apart. Passive avoidance tests were run following the previously described procedure.³² On the training day, each mouse ($n = 10\text{--}12$ mice/group) was placed inside the illuminated compartment facing away from the dark compartment. The door leading to the dark compartment was opened after a 60-s habituation period. When the animal had placed all four paws in the dark compartment, a footshock (0.5mA, 3s) was delivered and the animal was immediately removed from the apparatus and returned to its home cage. The time taken to enter the dark compartment (step-through latency) was recorded. Retention was tested 24h and 7 days later following the same procedure, but with no footshock. The maximum step-through latency lasted 300s.

2.8.3 | Hebb-Williams maze

This task was used for the advantages that it offers over other tests because not only can problem-solving, visuo-spatial abilities, and cognitive performance in rodents³³ be assessed, but so can easy and difficult learnings and, consequently, minor cognitive deficits can be differentiated. Motivation to perform this maze is not based on reinforcement (i.e., food), but on escaping from a stressful situation (cold water), which can influence learning and memory.^{34,35}

The maze used in our experiments was made of black plastic and measured 60cm wide × 60cm long × 10cm high. It contained a start box and a goal box (both 14cm wide × 9cm long), which were positioned in diagonally opposite corners. The maze contained cold water at a wading depth (15°C, 3.5cm high), while the goal box was stocked with fresh dry tissue. Several maze designs were produced by fixing different arrangements of barriers to a clear plastic ceiling. This apparatus allows the cognitive process of routed learning and water-escape motivation to be measured. The following procedure was based on that employed by,³⁶ in which mice must navigate the maze and cross over from the wet start box to the dry goal box to escape cold water. Animals ($n = 10\text{--}12$ mice/group) underwent a 5-min habituation period (dry sand, no barriers) on day 1, and faced problem A on day 2 and problem D on day 3 (4 trials/day) (practice mazes). Mice were subsequently submitted to mazes 1, 5, 3, 4, and 8 on separate days on which eight trials took place. The time limit for reaching the goal box was 5min, after which time the mouse was guided to the box. The following measurements were recorded: total latency score (the sum of the latencies in all the

problem trials in each maze); latency to reach the goal during the eighth trial; error scores, for which a similar total was used (where "error" was considered the act of entering the error zone as previously described). Following,³⁷ mazes were defined as easy (1, 3, and 4) or difficult (5 and 8).

2.9 | Statistical analysis

The results are reported as the mean \pm SEM. All the employed statistical parameters were calculated with SPSS v28. The Shapiro-Wilk test was used to test for data distribution normality. A one-way ANOVA or a two-way ANOVA was used as parametric tests, and the Mann-Whitney *U* test or the Kruskal-Wallis test was used as non-parametric alternatives. Values of $p < 0.05$ were considered statistically significant.

Electron microscopy imaging was analyzed with a one-way ANOVA. Quantitative RT-PCR and behavioral data from the novel object recognition were analyzed by a two-way ANOVA with two between-subject variables: ethanol (saline and ethanol); MSC-EVs (with and without EVs). Bonferroni adjustment was employed for the post hoc comparisons in the ANOVA. The number of errors in the Hebb-Williams maze data was analyzed by a two-way ANOVA with the same two between-subject variables in the easy and difficult mazes. As normal distribution was lacking, the time to reach the goal and the particular measures of each trial in the easy and difficult mazes of the Hebb-Williams maze, and the passive avoidance test data, were analyzed by the Kruskal-Wallis test and pairwise comparisons by the Mann-Whitney *U* test.

3 | RESULTS

3.1 | MSC-EVs ameliorate the neuroinflammatory immune response induced by binge-like ethanol treatment in adolescent mice

We first characterized MSC-EVs by electron microscopy, nanoparticle tracking analysis, and EVs markers (Figure 1). The size distribution and concentration of the MSC-secreted nanoparticles using the NanoSight resulted in a high peak that ranged between 100 and 200 nm, which included the size range of EVs as demonstrated by electron microscopy. In addition, these EVs expressed the exosome markers, named tetraspanin proteins (CD63, CD9, and CD81), whereas no signs of cytosolic protein contamination were observed by the calnexin protein.

Then we analyzed if MSC-EVs administration can restore the up-regulation in the mRNA levels of inflammatory genes induced by ethanol treatment. For these experiments, we used adipose MSC-EVs intravenously administered 3h before ethanol injection in adolescent mice (see 2. Materials and Methods). We measured the COX-2, NF- κ B, iNOS, CX3CL1, MIP-1 α , and MCP-1 levels in the PFC under different experimental conditions. Figure 2 shows that ethanol treatment increased the gene expression of COX-2 [$F(3, 36) = 12.541, p < 0.01$; Figure 2A], NF- κ B [$F(3, 36) = 21.753, p < 0.001$; Figure 2B], CX3CL1 [$F(3, 35) = 7.262, p < 0.01$; Figure 2D], MIP-1 α [$F(3, 35) = 20.902, p < 0.01$; Figure 2E] and MCP-1 [$F(3, 34) = 17.718, p < 0.01$; Figure 2F] compared to their saline counterparts. Notably, MSC-EVs administration was able to attenuate the ethanol-induced expression of these proinflammatory molecules compared to the

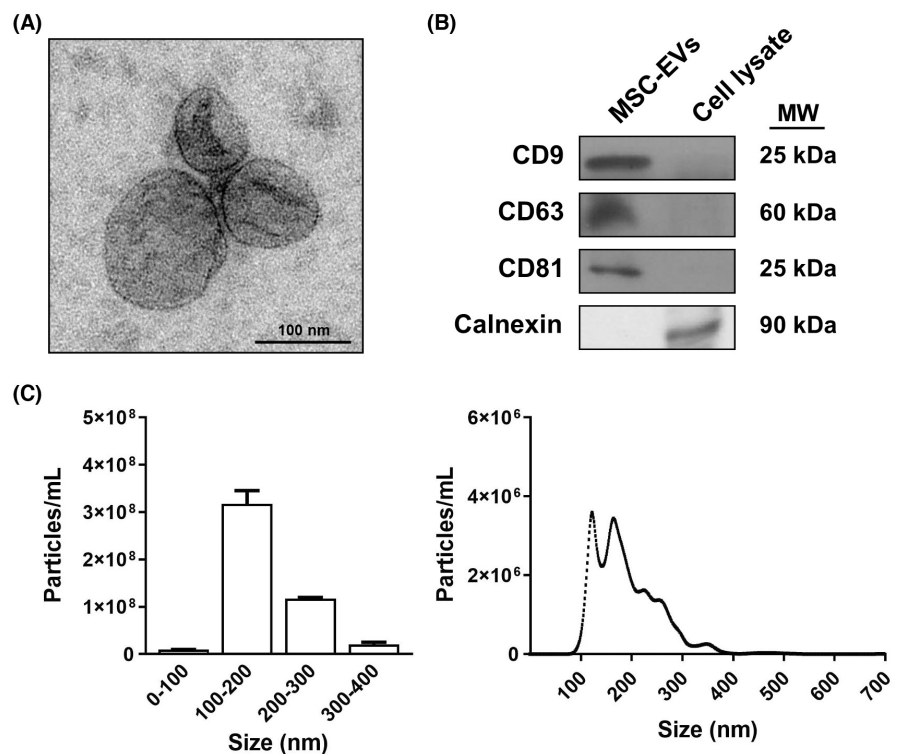


FIGURE 1 Characterization of MSC-EVs. (A) Electron microscopy image of MSC-EVs. (B) Analysis of the protein expression of EV markers, such as CD9, CD63, and CD81 in EVs and the cell lysate. Calnexin expression was also used to discard cytosolic protein contamination in EV samples. The cell lysate from the astrocytes in the culture was used as the positive control. A representative immunoblot for each protein is shown. (C) Measurement of the size distribution and concentration of MSC-EVs by the nanoparticles tracking analysis.

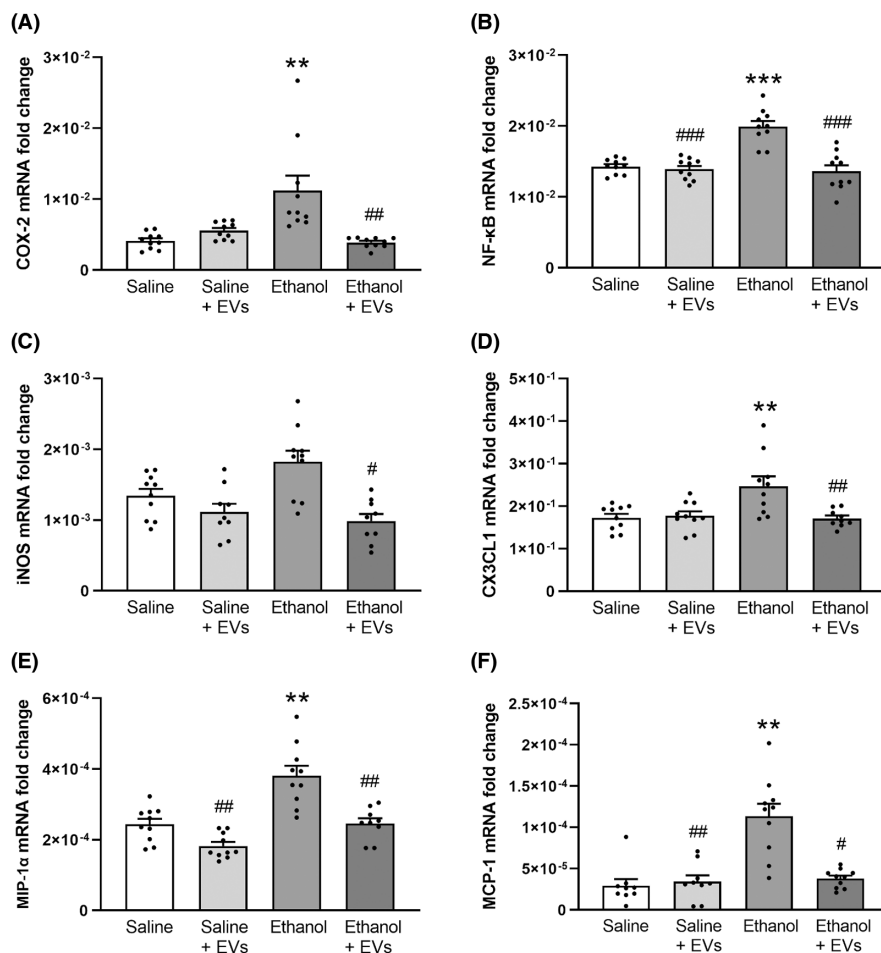


FIGURE 2 MSC-EVs restore the levels of inflammatory genes induced by binge-like ethanol treatment in adolescent mice. The mRNA levels of COX-2 (A), NF-κB (B), iNOS (C), CX3CL1 (D), MIP-1α (E), and MCP-1 (F) were analyzed in the PFC samples of adolescent mice. Data represent mean ± SEM, $n=9-10$ mice/group. ** $p < 0.01$ and *** $p < 0.001$, compared to their respective saline-treated group; # $p < 0.05$, ## $p < 0.01$, and ### $p < 0.001$, compared to their respective ethanol-treated group.

ethanol-treated mice COX-2 [$F(3, 36)=12.541, p < 0.01$; Figure 2A], NF-κB [$F(3, 36)=21.753, p < 0.001$; Figure 2B], CX3CL1 [$F(3, 35)=7.262, p < 0.01$; Figure 2D], MIP-1α [$F(3, 35)=20.902, p < 0.01$; Figure 2E] and MCP-1 [$F(3, 34)=17.718, p < 0.05$; Figure 2F]. However, iNOS expression (Figure 2C) showed a tendency to increase in the ethanol-treated mice. This expression significantly decreased in the animals treated with ethanol plus MSC-EVs compared to the ethanol-treated mice [$F(3, 34)=7.541, p < 0.05$]. In addition, ethanol treatment significantly increased the NF-κB [$F(3, 36)=21.753, p < 0.001$; Figure 2B], MIP-1α [$F(3, 35)=20.902, p < 0.01$; Figure 2E] and MCP-1 [$F(3, 34)=17.718, p < 0.01$; Figure 2F] levels compared to the saline plus MSC-EVs-treated mice. No changes in the expression of these genes were found between the saline- and MSC-EVs-treated animals.

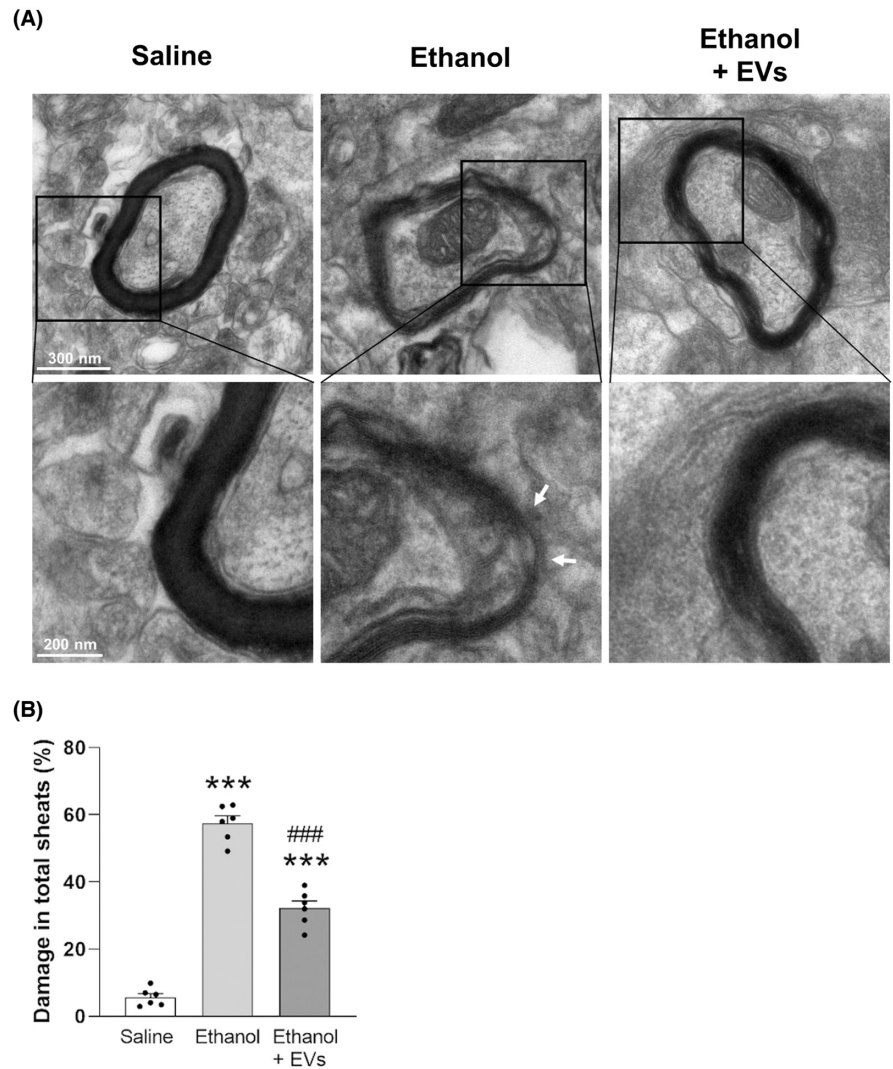
3.2 | MSC-EVs reduce the myelin and synaptic alterations in the PFC of ethanol-treated adolescent mice

Considering that intermittent binge-like ethanol drinking alters the myelin structure in the PFC of adolescent mice,¹⁸ we herein analyzed the potential beneficial role of MSC-EVs in ethanol-induced myelin structure alterations. Figure 3A shows that while ethanol

treatment induces the irregular shapes of myelin fibers and causes interlaminar splitting of myelin sheaths (Figure 3A, arrows), the administration of MSC-EVs ameliorates the ethanol effects. Likewise, the analysis of damage in the total myelin sheaths increased in the animals treated with ethanol [$F(2, 15)=190.940, p < 0.001$], whereas the MSC-EVs injection was able to restore this alteration in ethanol-treated mice [$F(2, 15)=190.940, p < 0.001$; Figure 3B]. However, significant differences in the total myelin sheaths were observed between the animals treated with saline and ethanol plus MSC-EVs [$F(2, 15)=190.940, p < 0.001$]. We next determined the expression of several myelin-related genes in the PFC of the adolescent mice treated with ethanol and/or MSC-EVs. Figure 4 shows that EVs administration was able to restore the decrease in the gene expression of CNPase [$F(3, 35)=40.804, p < 0.001$; Figure 4A], MAG [$F(3, 34)=28.772, p < 0.001$; Figure 4B] and MBP [$F(3, 35)=17.747, p < 0.01$; Figure 4C] induced by ethanol in adolescent mice. Nonetheless, NG2 expression (Figure 4D) showed a tendency to decrease in the ethanol-treated mice, and its expression significantly increased in the animals treated with ethanol plus MSC-EVs compared to the ethanol-treated mice [$F(3, 32)=14.423, p < 0.001$]. However, no changes were found in the expression of these genes between the saline-treated and EVs-treated animals.

We also assessed the potential role of MSC-EVs in the ultrastructural alterations in the synaptic elements induced by intermittent

FIGURE 3 MSC-EVs diminish the myelin sheath disarrangements induced by binge-like ethanol treatment in adolescent mice. (A) The representative transmission electron micrographs of the PFC of the adolescent mice treated with saline, ethanol, and ethanol plus EVs are shown. Arrows indicate the interlaminar splitting of myelin sheaths. (B) Bars represent the percentage of myelin sheath damage. Data denote mean \pm SEM, $n=6$ mice/group. *** $p < 0.001$, compared to the saline-treated group, ### $p < 0.001$, compared to the ethanol-treated group.



ethanol treatment in adolescent mice (Figure 5A), as previously demonstrated.¹⁸ To accomplish this, we analyzed vesicle number, synaptic cleft width, and postsynaptic density thickness in the PFC of adolescent mice. Figure 5 shows that MSC-EVs were able to restore: (1) decreases in the number of vesicles [$F(2, 15)=57.275$, $p < 0.001$; Figure 5B]; (2) reduction in postsynaptic density thickness [$F(2, 15)=7.840$, $p < 0.05$; Figure 5C]; (3) increases in synaptic cleft width [$F(2, 15)=29.120$, $p < 0.001$; Figure 5D] in the ethanol-treated adolescent mice number of vesicles [$F(2, 15)=57.280$, $p < 0.001$; Figure 5B], postsynaptic density thickness [$F(2, 15)=7.840$, $p < 0.01$; Figure 5C] and synaptic cleft width [$F(2, 15)=29.120$, $p < 0.001$; Figure 5D]. No significant differences were noted between the animals treated with saline and ethanol plus EVs.

3.3 | MSC-EVs restore the cognitive dysfunctions induced by binge-like ethanol treatment in adolescent mice

We next assessed whether the amelioration of the neuroinflammation, myelin and synaptic alterations induced by MSC-EVs in the

ethanol-treated adolescent mice would also be capable of restoring cognitive dysfunction. We performed several memory and learning tasks, such as the passive avoidance test, the novel object recognition test, and Hebb-Williams maze. These paradigms have been validated and used fairly often in animal cognitive research, to evaluate cognitive aspects, such as recognition ability, short-term/working memory, short-term and long-term memory, and also the learning process.^{18,32,38-41}

In the novel object recognition test (Figure 6A), the two-way ANOVA revealed a significant effect of the variables Ethanol [$F(1, 43)=4.487$, $p < 0.05$], MSC-EVs [$F(1, 43)=4.482$, $p < 0.05$], and of the Ethanol \times MSC-EVs interaction [$F(1, 43)=6.006$, $p = 0.01$]. The ethanol-treated mice failed to recognize the novel object because their discrimination index was significantly lower than in the saline-treated mice and the mice treated with MSC-EVs plus ethanol ($p < 0.01$ in both cases).

The Kruskal-Wallis test for the passive avoidance data (Figure 6B) showed an effect on the training day [$\chi^2(2)=12.440$, $p < 0.01$] and 7 days after the training day [$\chi^2(2)=17.359$, $p < 0.001$]. On the training day, the Mann-Whitney U test revealed longer latency to cross to the dark compartment in the animals treated

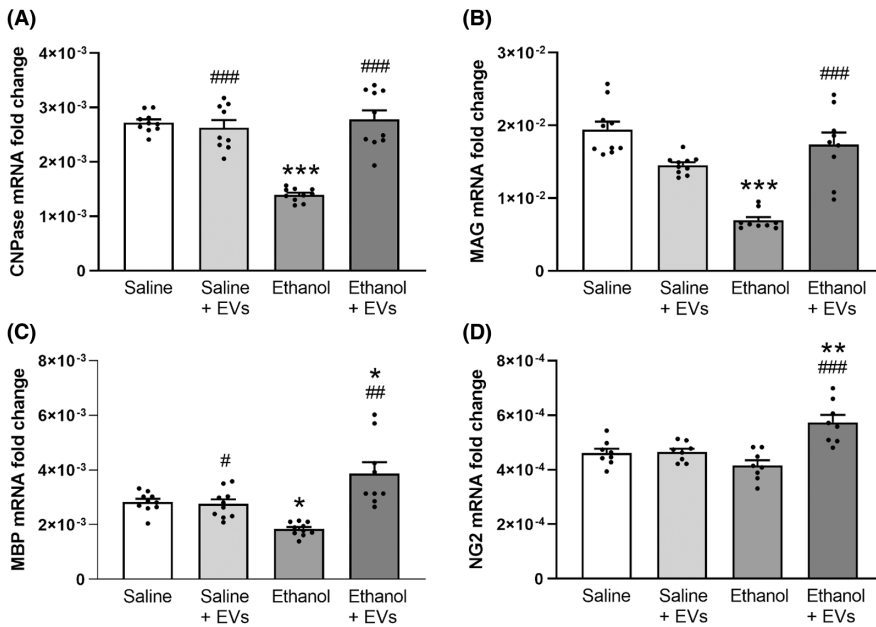


FIGURE 4 MSC-EVs restore the levels of the myelin-related genes induced by binge-like ethanol treatment in adolescent mice. The mRNA levels of CNPase (A), MAG (B), MBP (C), and NG2 (D) were analyzed in the PFC samples of adolescent mice. Data represent mean ± SEM, $n=9-10$ mice/group. * $p < 0.05$, ** $p < 0.01$ and *** $p < 0.001$, compared to their respective saline-treated group; # $p < 0.05$, ## $p < 0.01$ and ### $p < 0.001$, compared to their respective ethanol-treated group.

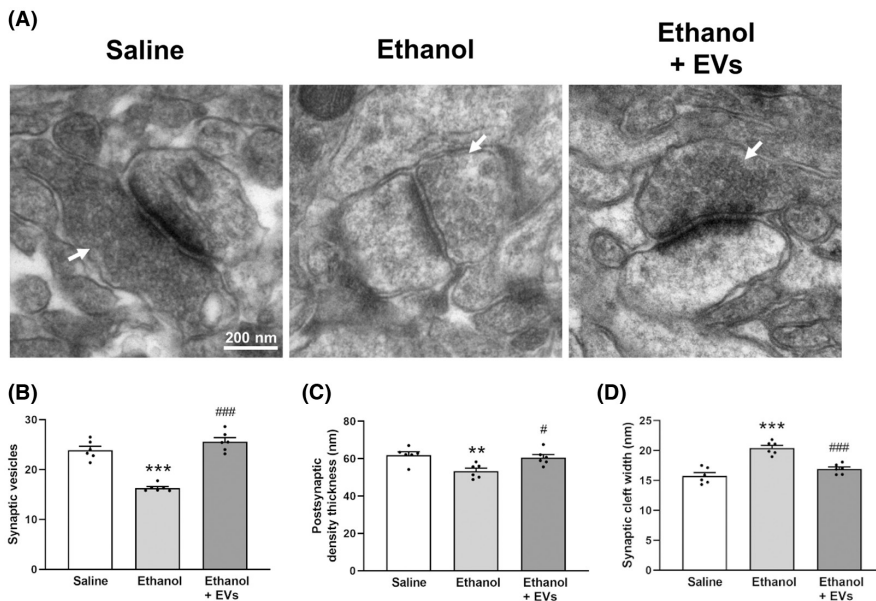


FIGURE 5 The electron microscopy analysis shows the role of MSC-EVs in the synaptic structure induced by binge-like ethanol treatment in adolescent mice. (A) Representative transmission electron micrographs from the PFC of the adolescent mice treated with saline, ethanol, and ethanol plus EVs. Arrows mark vesicles. Bars represent synaptic vesicle number (B), postsynaptic density thickness (C), and synaptic cleft width (D). Data represent mean ± SEM, $n=6$ mice/group. ** $p < 0.01$ and *** $p < 0.001$, compared to their respective saline-treated group; # $p < 0.05$ and ### $p < 0.001$, compared to their respective ethanol-treated group.

with ethanol compared to all the other experimental groups (saline: $U=23$, $p=0.01$; ethanol plus MSC-EVs: $U=17$, $p < 0.01$; saline plus MSC-EVs $U=10$, $p < 0.001$). Conversely, 7 days after the training day, the ethanol-treated mice crossed to the dark compartment more quickly than all other groups (saline: $U=10.5$, $p < 0.001$; ethanol plus MSC-EVs: $U=7.5$, $p < 0.001$; saline plus MSC-EVs: $U=23$, $p < 0.05$). These findings suggest that ethanol causes poor retention in memory tasks, while MSC-EVs administration can preserve cognition when harmful ethanol effects come into play.

The Kruskal-Wallis test revealed an effect on the time to reach the goal in the easy and difficult mazes [$\chi^2(2)=24.500$, $p < 0.01$; $\chi^2(2)=13.500$, $p=0.001$, respectively; Figure 6C]. Pairwise comparisons showed that the ethanol-treated mice took longer to reach the goal in the easy and difficult mazes compared to the other

experimental groups (saline: $U=24.5$, $p < 0.01$; ethanol plus MSC-EVs: $U=35.3$, $p < 0.05$; saline plus MSC-EVs: $U=27$, $p < 0.05$, in the easy mazes; and saline: $U=13.5$, $p < 0.001$; ethanol plus MSC-EVs: $U=13$, $p < 0.01$; saline plus MSC-EVs: $U=11$, $p=0.001$, in the difficult mazes). These data (Figure 6C) and the data from Supplementary Material (Figures S2 and S3) also confirm that MSC-EVs treatment was able to revert the impairment in the spatial learning induced by ethanol in adolescent mice.

Furthermore, the ANOVA for the total number of errors in the Hebb-Williams maze (Figure 6D) revealed an effect of the variable Ethanol in the easy [$F(1, 39)=5.785$, $p < 0.05$] and difficult [$F(1, 39)=47.493$, $p < 0.001$] mazes. The animals treated with ethanol and ethanol plus MSC-EVs made more errors while learning mazes versus the saline-treated mice ($p < 0.01$ and $p < 0.001$ for the easy and difficult mazes, respectively; Figure 6D and Figure S4).

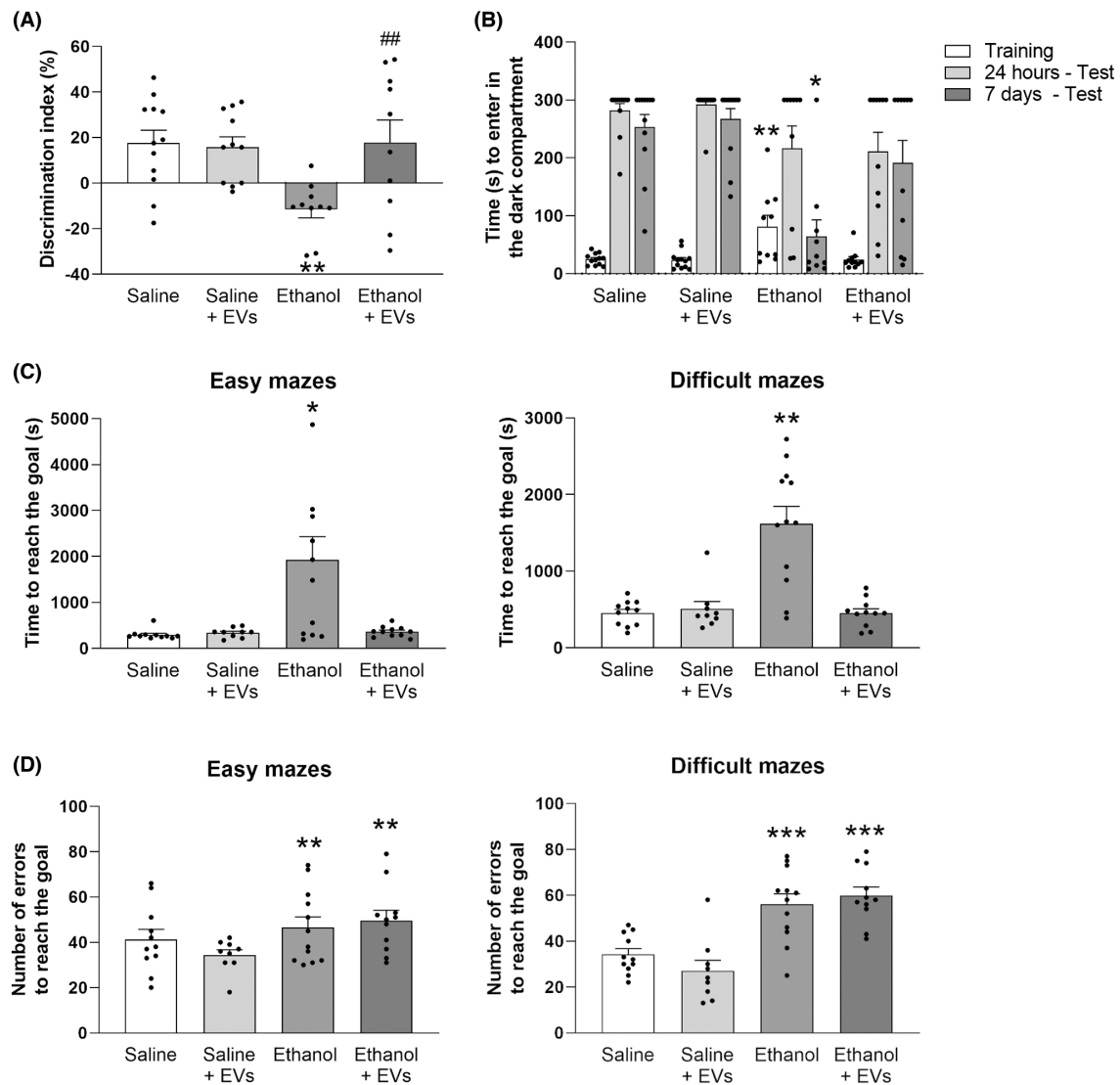


FIGURE 6 MSC-EVs restore ethanol-induced cognitive dysfunction in adolescent mice. (A) Bars represent the mean (\pm SEM, $n = 10-12$ mice/group) of the discrimination index during the novel object recognition task. $**p < 0.01$ compared to their respective saline-treated group. $##p < 0.01$ compared to the ethanol-treated group. (B) Bars represent the time taken to enter the dark compartment of the passive avoidance test during the training and test sessions (24 h and 7 days after training). Data are presented as mean (\pm SEM), $n = 10-12$ mice/group. $*p < 0.05$ and $**p < 0.01$, compared to all the other experimental groups. (C) Bars represent the mean (\pm SEM, $n = 10-12$ mice/group) of the time to reach the goal in the difficult and easy mazes in Hebb-Williams mazes. $*p < 0.05$ and $**p < 0.01$, compared to all the other experimental groups. (D) Bars denote the mean (\pm SEM, $n = 10-12$ mice/group) of the number of errors to reach the goal in the difficult and easy mazes in Hebb-Williams mazes. $**p < 0.01$ and $***p < 0.001$, compared to their respective saline-treated group.

3.4 | Role of MSC-EVs in the ethanol-induced inflammatory response in astroglial cells in primary culture

We have previously demonstrated that ethanol induces neuroinflammation by activating the TLR4 inflammatory response in glial cells.^{17,42} Therefore, to extend the *in vivo* results on the protective role of MSC-EVs in ethanol-induced neuroinflammation, we also used the primary culture of the astroglial cells exposed to ethanol and treated with and without MSC-EVs. The results demonstrated that ethanol treatment increased the levels of several proinflammatory genes, such as TLR4, NF- κ B, iNOS, CX3CL1, and MIP-1 α .

The one-way ANOVA revealed that ethanol treatment increased the gene expression of TLR4 [$F(3, 13) = 6.663$, $p < 0.05$; Figure 7A], NF- κ B [$F(3, 14) = 13.360$, $p < 0.05$; Figure 7B], iNOS [$F(3, 13) = 6.363$, $p < 0.05$; Figure 7C], CX3CL1 [$F(3, 15) = 39.440$, $p < 0.01$; Figure 7D] and MIP-1 α [$F(3, 16) = 30.990$, $p < 0.001$; Figure 7E]. Notably, the treatment with MSC-EVs significantly diminished the genes expression induced by ethanol TLR4 [$F(3, 13) = 6.663$, $p < 0.05$; Figure 7A], NF- κ B [$F(3, 14) = 13.360$, $p < 0.01$; Figure 7B], iNOS [$F(3, 13) = 6.363$, $p < 0.01$; Figure 7C], CX3CL1 [$F(3, 15) = 39.440$, $p < 0.001$; Figure 7D] and MIP-1 α [$F(3, 16) = 30.990$, $p < 0.001$; Figure 7E]. No significant changes were observed in the expression of these inflammatory genes when MSC-EVs were added to the cell medium alone.

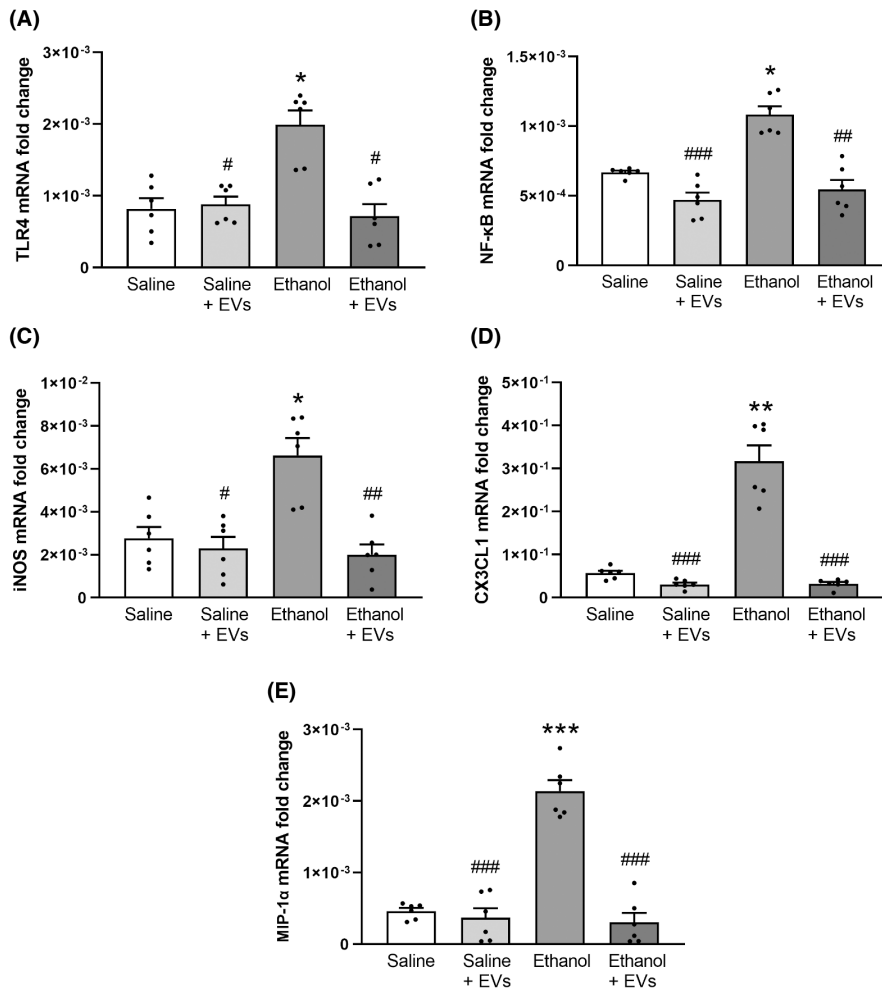


FIGURE 7 MSC-EVs lower the levels of the inflammatory genes induced by ethanol treatment in astroglial cells. The astrocytes in primary culture treated or not with ethanol in the presence or absence of MSC-EVs were used to analyze the mRNA levels of TLR4 (A), NF-κB (B), iNOS (C), CX3CL1 (D) and MIP-1α (E). Data represent mean ± SEM ($n=6$ independent experiments). * $p < 0.05$, ** $p < 0.01$ and *** $p < 0.001$, compared to their respective untreated cells; # $p < 0.05$, ## $p < 0.01$ and ### $p < 0.001$, compared to their respective ethanol-treated cells.

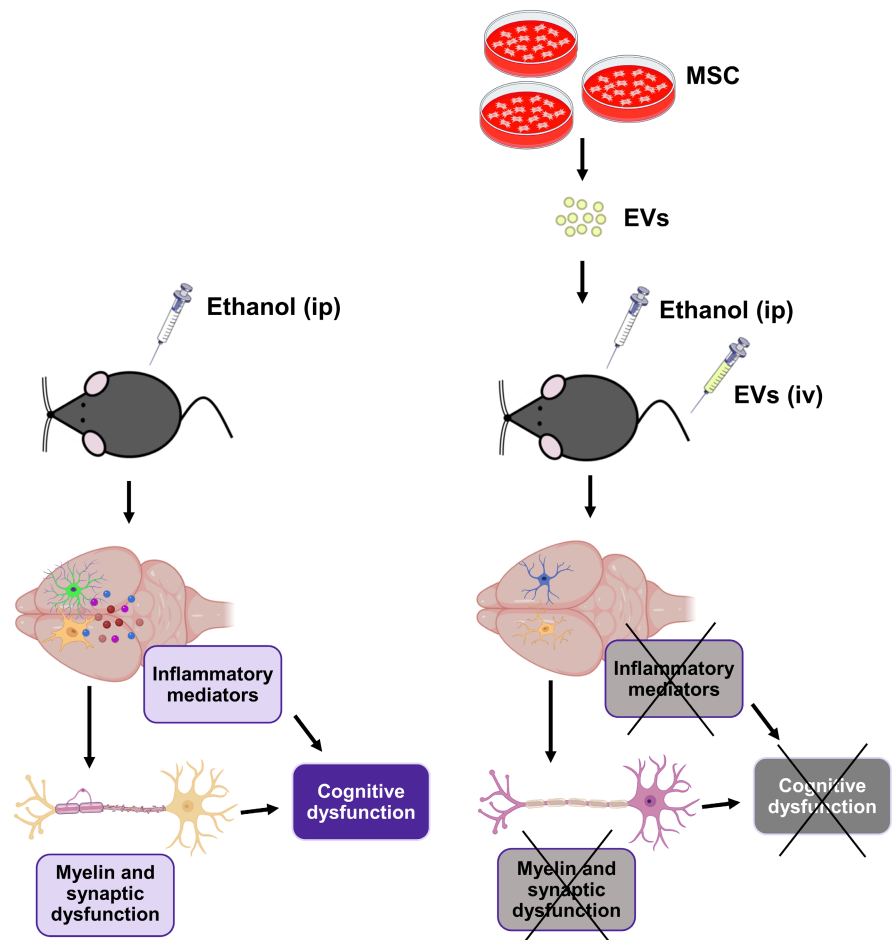
4 | DISCUSSION

We have previously demonstrated the critical role of the innate immune response in the ethanol-induced PFC damage and cognitive dysfunctions induced by binge-like ethanol exposure in adolescence.^{18,25} Considering the regenerative potential of MSC-EVs in both brain damage and neurodegenerative disorders,^{43–46} MSC-EVs were herein used to ameliorate the neuroinflammation induced by binge ethanol drinking. The present findings provide evidence that MSC-EVs administration mostly restores the neuroinflammatory response, along with myelin and synaptic structural alterations, as well as cognitive and memory dysfunctions induced by binge-like ethanol treatment in adolescent mice (Figure 8).

Our previous studies revealed the role of EVs as amplifiers of the TLR4 response and the neuroinflammation induced by ethanol treatment in astroglial cells in culture³⁰ and in in vivo brain tissue.⁴⁷ However, different recent studies also report the potential role of EVs to show that EVs emerge as therapeutic agents of different diseases, such as neurodegenerative disorders and brain damage. Experimental studies have specifically evidenced the anti-inflammatory and antioxidative properties of MSC-EVs in the TLR4 activation induced by its specific ligand, lipopolysaccharide (LPS). For instance, MSC-EVs prevent LPS-induced microglia activation and the production of

inflammatory mediators in rats⁴⁴ and microglial cells.⁴⁸ Han et al.⁴⁹ have shown that MSC-EVs alleviate the brain expression of inflammatory cytokines in rats with subarachnoid hemorrhage by inhibiting the activation of nuclear transcription factor NF-κB. In line with these findings, we show that MSC-EVs can prevent the up-regulation of the expression of inflammatory genes (e.g., iNOS, MIP-1α, NF-κB, and CX3CL1) induced by binge-like ethanol treatment in both the adolescent PFC and ethanol-treated astroglial cells. Similarly, Ezquer et al.⁵⁰ have demonstrated that MSC-EVs inhibit the neuroinflammation and glial activation induced by chronic alcohol consumption. Protective functions of these microvesicles have been shown by the miRNAs contained in MSC-EVs, which modulate various cell signaling processes and regulate the expression of multiple target genes with antioxidative and anti-inflammatory properties.⁵¹ Other studies have also demonstrated that MSC-EVs perform immunosuppressive functions by decreasing T- and B-cell proliferation, by releasing immunomodulating factors (e.g., iNOS, PGE2, TSG-6, and HLA-G) packed in EVs.⁵² Conversely, the EVs derived by ethanol-treated astrocytes could be internalized by neurons to increase the levels of proinflammatory molecules, by compromising their survival.³⁰ However, the present study confirms that the systemic administration of MSC-EVs exerts anti-inflammatory properties in ethanol-treated adolescent mice. Indeed, MSC-EVs incorporated into glial cells and neurons could promote

FIGURE 8 Schematic representation of the protective effects of MSC-EVs administration on ethanol-induced neuroinflammation. Adipose tissue-derived EVs were administered by intravenous injection (iv) prior to ethanol treatment (ip, intraperitoneal injection) in adolescent mice. MSC-EVs administration ameliorates ethanol-induced up-regulation in inflammatory genes in the prefrontal cortex of adolescent mice. Notably, MSC-EVs treatment also restored the myelin and synaptic derangements, as well as the memory and learning impairments, induced by ethanol administration.



neuroprotection against the neuroinflammatory response and brain damage.^{49,53,54}

Adolescence is a critical brain maturation period when neurotoxic ethanol effects can induce structural cortical alterations in humans^{55,56} and experimental models,¹⁸ which could be associated with persistent neurobehavioral deficits, including memory and cognitive dysfunction.^{18,57,58} The present findings show that the intravenous MSC-EVs injection into binge ethanol-treated adolescent mice is able to reduce both alterations in white matter (e.g., irregular myelin fiber shapes, interlaminar splitting of myelin sheaths) and ultrastructural changes in synapses, such as a reduction in both postsynaptic thickness and synaptic vesicle number. In line with our results, a study in rhesus monkeys with cortical injury has reported that MSC-EVs administration can promote therapeutic actions through the recovery of the structure of premotor pyramidal neurons and dendritic plasticity function.⁵⁹ Treating brain injury with MSC-EVs can also promote the restoration of long-term perinatal microstructural abnormalities of white matter,⁴⁴ and remyelination by acting directly on oligodendrocyte progenitor cells and indirectly on microglia activation.⁴⁶ Therefore, these protective and supportive effects of MSC-EVs can be attributed not only to their anti-inflammatory properties,⁴⁴ but also to the up-regulation of myelin-related genes⁶⁰ and neural growth factors (i.e., BDNF, VEGF, and EGF)⁶¹ in brain injury.

We have previously demonstrated that alterations in myelin and synaptic structures induced by binge drinking in adolescence can lead to poor synaptic transmission efficacy, which causes cognitive impairments in adolescent mice.¹⁸ Recent reports show the involvement of MSC-EVs in the protection of LPS-induced spatio-temporal memory deficits and learning impairments as assessed by a novel object recognition test and Barnes maze.⁴⁴ Cognitive function restoration using MSC-EVs has also been demonstrated in animal models of neurodegenerative diseases, such as Alzheimer's disease, brain injury, Parkinson's disease, schizophrenia, among others.^{43,45,46} Notably, the present study demonstrates that MSC-EVs ameliorate ethanol-induced spatio-temporal memory dysfunction, as well as learning and recognition memory deficits as evaluated by the novel object recognition test, the passive avoidance task, and Hebb-Williams maze. Indeed, we show that MSC-EVs administration is capable of normalizing the disability to recognize the novel object, the shorter latency time during the passive avoidance test, and the longer times to complete the Hebb-Williams mazes in adolescent mice treated with ethanol. Therefore, we hypothesize that an intravenous MSC-EVs injection may rescue cognitive deficits by regulating inflammatory responses and structural cortical alterations. Several studies suggest that the protective role of MSC-EVs in cognitive deficits could be attributed to the amelioration of white matter disturbances,⁴⁴

along with the morphological changes in spine density and dendritic intersections or calcium signaling alterations.⁶² The fact that the stronger effect of MSC-EVs on the ethanol-treated mice was observed in Hebb-Williams maze for the time to reach the goal, and not for the number of made errors, could be subjected to MSC-EVs, which were unable to restore behavioral impairments by altering flexibility in strategy selection for problem-solving.⁶³ These deficits are more evident in very complex tasks, such as Hebb-Williams mazes.⁶⁴ Indeed Match et al.⁶⁵ showed that adolescent rats treated with ethanol repeated the same incorrect response in succession, unlike the controls, which suggests lack of flexibility in correcting incorrect choices within a short timeframe.

Taken together, these novel results support the protective role of MSC-EVs in not only the neuroinflammatory immune response, but also in the alterations of myelin and synaptic structures and cognitive dysfunction induced by binge-like ethanol treatment in adolescence. These findings evidence the therapeutic potential of MSC-EVs and may provide a new tool to treat the neuroinflammation associated with alcohol consumption and other neurodegenerative diseases.

ACKNOWLEDGMENTS

The authors thank L. Jareño for her contribution to some experiments. We also thank the Electron Microscopy at the Príncipe Felipe Research Center. This work has been supported by grants from the Spanish Ministry of Health-PNSD (2018-I003 and 2019-I039), GVA (CIAICO/2021/203), GVA (CIPROM/2021/080), the Carlos III Institute and FEDER funds (RTA-Network, RD16/0017/0004), the Primary Addiction Care Research Network (RD21/0009/0005) and FEDER Funds, GVA.

CONFLICT OF INTEREST STATEMENT

The authors have no conflicts of interest to declare.

DATA AVAILABILITY STATEMENT

The data that support the findings of this study are available on request from the corresponding author. The data are not publicly available due to privacy or ethical restrictions.

ORCID

María Pascual  <https://orcid.org/0000-0003-1420-631X>

REFERENCES

- Fujita Y, Kadota T, Araya J, Ochiya T, Kuwano K. Clinical application of mesenchymal stem cell-derived extracellular vesicle-based therapeutics for inflammatory lung diseases. *J Clin Med*. 2018;7(10):E355.
- Akyurekli C, Le Y, Richardson RB, Fergusson D, Tay J, Allan DS. A systematic review of preclinical studies on the therapeutic potential of mesenchymal stromal cell-derived microvesicles. *Stem Cell Rev Rep*. 2015;11(1):150-160.
- Janockova J, Slovinska L, Harvanova D, Spakova T, Rosocha J. New therapeutic approaches of mesenchymal stem cells-derived exosomes. *J Biomed Sci*. 2021;28(1):39.
- Hu Q, Lyon CJ, Fletcher JK, Tang W, Wan M, Hu TY. Extracellular vesicle activities regulating macrophage- and tissue-mediated injury and repair responses. *Acta Pharm Sin B*. 2021;11(6):1493-1512.
- Varderdou-Minasian S, Lorenowicz MJ. Mesenchymal stromal/stem cell-derived extracellular vesicles in tissue repair: challenges and opportunities. *Theranostics*. 2020;10(13):5979-5997.
- Zhu F, Chong Lee Shin OLS, Pei G, et al. Adipose-derived mesenchymal stem cells employed exosomes to attenuate AKI-CKD transition through tubular epithelial cell dependent Sox9 activation. *Oncotarget*. 2017;8(41):70707-70726.
- Pascual M, Ibáñez F, Guerri C. Exosomes as mediators of neuroglia communication in neuroinflammation. *Neural Regen Res*. 2019;15(5):796-801.
- Rashed MH, Bayraktar E, Helal GK, et al. Exosomes: from garbage bins to promising therapeutic targets. *Int J Mol Sci*. 2017;18(3):E538.
- Wang J, Sun X, Zhao J, et al. Exosomes: a novel strategy for treatment and prevention of diseases. *Front Pharmacol*. 2017;8:300.
- Yari H, Mikhailova MV, Mardasi M, et al. Emerging role of mesenchymal stromal cells (MSCs)-derived exosome in neurodegeneration-associated conditions: a groundbreaking cell-free approach. *Stem Cell Res Ther*. 2022;13(1):423.
- Steinberg L. Cognitive and affective development in adolescence. *Trends Cogn Sci*. 2005;9(2):69-74.
- Alfonso-Loeches S, Guerri C. Molecular and behavioral aspects of the actions of alcohol on the adult and developing brain. *Crit Rev Clin Lab Sci*. 2011;48(1):19-47.
- Casey BJ, Jones RM, Hare TA. The adolescent brain. *Ann N Y Acad Sci*. 2008;1124:111-126.
- Guerri C, Pascual M. Impact of neuroimmune activation induced by alcohol or drug abuse on adolescent brain development. *Int J Dev Neurosci*. 2019;77:89-98.
- Jacobus J, Tapert SF. Neurotoxic effects of alcohol in adolescence. *Annu Rev Clin Psychol*. 2013;9:703-721. doi:10.1146/annurev-clinpsy-050212-185610
- Alfonso-Loeches S, Pascual-Lucas M, Blanco AM, Sanchez-Vera I, Guerri C. Pivotal role of TLR4 receptors in alcohol-induced neuroinflammation and brain damage. *J Neurosci*. 2010;30(24):8285-8295.
- Fernandez-Lizarbe S, Pascual M, Guerri C. Critical role of TLR4 response in the activation of microglia induced by ethanol. *J Immunol*. 2009;183(7):4733-4744.
- Montesinos J, Pascual M, Pla A, et al. TLR4 elimination prevents synaptic and myelin alterations and long-term cognitive dysfunctions in adolescent mice with intermittent ethanol treatment. *Brain Behav Immun*. 2015;45:233-244.
- Friedman NP, Robbins TW. The role of prefrontal cortex in cognitive control and executive function. *Neuropsychopharmacology*. 2022;47(1):72-89.
- Tapert SF, Ozyurt SS, Myers MG, Brown SA. Neurocognitive ability in adults coping with alcohol and drug relapse temptations. *Am J Drug Alcohol Abuse*. 2004;30(2):445-460.
- Yin K, Wang S, Zhao RC. Exosomes from mesenchymal stem/stromal cells: a new therapeutic paradigm. *Biomark Res*. 2019;7:8.
- Mellado-López M, Griffeth RJ, Meseguer-Ripolles J, Cugat R, García M, Moreno-Manzano V. Plasma rich in growth factors induces cell proliferation, migration, differentiation, and cell survival of adipose-derived stem cells. *Stem Cells Int*. 2017;2017:5946527-5946511.
- Muñoz-Criado I, Meseguer-Ripolles J, Mellado-López M, et al. Human suprapatellar fat pad-derived mesenchymal stem cells induce chondrogenesis and cartilage repair in a model of severe osteoarthritis. *Stem Cells Int*. 2017;2017:4758930-4758912.
- Brust V, Schindler PM, Lewejohann L. Lifetime development of behavioural phenotype in the house mouse (*Mus musculus*). *Front Zool*. 2015;12(Suppl 1):S17.

25. Pascual M, Blanco AM, Cauli O, Miñarro J, Guerri C. Intermittent ethanol exposure induces inflammatory brain damage and causes long-term behavioural alterations in adolescent rats. *Eur J Neurosci*. 2007;25(2):541-550.
26. Allen-Worthington KH, Brice AK, Marx JO, Hankenson FC. Intraperitoneal injection of ethanol for the euthanasia of laboratory mice (*Mus musculus*) and rats (*Rattus norvegicus*). *J Am Assoc Lab Anim Sci*. 2015;54(6):769-778.
27. Harris JA, Mihalas S, Hirokawa KE, et al. Hierarchical organization of cortical and thalamic connectivity. *Nature*. 2019;575(7781):195-202.
28. Le Merre P, Åhrlund-Richter S, Carlén M. The mouse prefrontal cortex: unity in diversity. *Neuron*. 2021;109(12):1925-1944.
29. Pascual M, Guerri C. The peptide NAP promotes neuronal growth and differentiation through extracellular signal-regulated protein kinase and Akt pathways, and protects neurons cocultured with astrocytes damaged by ethanol. *J Neurochem*. 2007;103(2):557-568.
30. Ibáñez F, Montesinos J, Ureña-Peralta JR, Guerri C, Pascual M. TLR4 participates in the transmission of ethanol-induced neuroinflammation via astrocyte-derived extracellular vesicles. *J Neuroinflammation*. 2019;16:136.
31. Schmittgen TD, Livak KJ. Analyzing real-time PCR data by the comparative C(T) method. *Nat Protoc*. 2008;3(6):1101-1108.
32. Pascual M, López-Hidalgo R, Montagud-Romero S, Ureña-Peralta JR, Rodríguez-Arias M, Guerri C. Role of mTOR-regulated autophagy in spine pruning defects and memory impairments induced by binge-like ethanol treatment in adolescent mice. *Brain Pathol*. 2021;31(1):174-188.
33. Rabinovitch MS, Rosvold HE. A closed-field intelligence test for rats. *Can J Psychol*. 1951;5(3):122-128.
34. Harris KM, Jensen FE, Tsao B. Three-dimensional structure of dendritic spines and synapses in rat hippocampus (CA1) at postnatal day 15 and adult ages: implications for the maturation of synaptic physiology and long-term potentiation. *J Neurosci*. 1992;12(7):2685-2705.
35. Moreira PS, Almeida PR, Leite-Almeida H, Sousa N, Costa P. Impact of chronic stress protocols in learning and memory in rodents: systematic review and meta-analysis. *PLoS One*. 2016;11(9):e0163245.
36. Fuchsberger T, Yuste R, Martínez-Bellver S, et al. Oral monosodium glutamate administration causes early onset of Alzheimer's disease-like pathophysiology in APP/PS1 mice. *J Alzheimers Dis*. 2019;72(3):957-975.
37. Stanford L, Brown RE. MHC-congenic mice (C57BL/6J and B6-H-2K) show differences in speed but not accuracy in learning the Hebb-Williams maze. *Behav Brain Res*. 2003;144(1-2):187-197.
38. Pascual M, Montesinos J, Montagud-Romero S, et al. TLR4 response mediates ethanol-induced neurodevelopment alterations in a model of fetal alcohol spectrum disorders. *J Neuroinflammation*. 2017;14(1):145.
39. Ródenas-González F, Blanco-Gandía MC, Miñarro J, Rodríguez-Arias M. Cognitive profile of male mice exposed to a ketogenic diet. *Physiol Behav*. 2022;254:113883.
40. Blanco-Gandía MC, Miñarro J, Rodríguez-Arias M. Behavioral profile of intermittent vs continuous access to a high fat diet during adolescence. *Behav Brain Res*. 2019;368:111891.
41. Blanco-Gandía MC, Montagud-Romero S, Navarro-Zaragoza J, et al. Pharmacological modulation of the behavioral effects of social defeat in memory and learning in male mice. *Psychopharmacology*. 2019;236(9):2797-2810.
42. Blanco AM, Vallés SL, Pascual M, Guerri C. Involvement of TLR4/type I IL-1 receptor signaling in the induction of inflammatory mediators and cell death induced by ethanol in cultured astrocytes. *J Immunol*. 2005;175(10):6893-6899.
43. Cui GH, Guo HD, Li H, et al. RVG-modified exosomes derived from mesenchymal stem cells rescue memory deficits by regulating inflammatory responses in a mouse model of Alzheimer's disease. *Immun Ageing*. 2019;16:10.
44. Drommelschmidt K, Serdar M, Bendix I, et al. Mesenchymal stem cell-derived extracellular vesicles ameliorate inflammation-induced preterm brain injury. *Brain Behav Immun*. 2017;60:220-232.
45. Harrell CR, Volarevic A, Djonov V, Volarevic V. Mesenchymal stem cell-derived exosomes as new remedy for the treatment of neurocognitive disorders. *Int J Mol Sci*. 2021;22(3):1433.
46. Zhang J, Buller BA, Zhang ZG, et al. Exosomes derived from bone marrow mesenchymal stromal cells promote remyelination and reduce neuroinflammation in the demyelinating central nervous system. *Exp Neurol*. 2022;347:113895.
47. Ibáñez F, Montesinos J, Area-Gomez E, Guerri C, Pascual M. Ethanol induces extracellular vesicle secretion by altering lipid metabolism through the mitochondria-associated ER membranes and sphingomyelinases. *Int J Mol Sci*. 2021;22(16):8438.
48. Jaimes Y, Naaldijk Y, Wenk K, Leovsky C, Emmrich F. Mesenchymal stem cell-derived microvesicles modulate lipopolysaccharide-induced inflammatory responses to microglia cells. *Stem Cells*. 2017;35(3):812-823.
49. Han M, Cao Y, Guo X, et al. Mesenchymal stem cell-derived extracellular vesicles promote microglial M2 polarization after subarachnoid hemorrhage in rats and involve the AMPK/NF- κ B signaling pathway. *Biomed Pharmacother*. 2021;133:111048.
50. Ezquer F, Quintanilla ME, Morales P, et al. Intranasal delivery of mesenchymal stem cell-derived exosomes reduces oxidative stress and markedly inhibits ethanol consumption and post-deprivation relapse drinking. *Addict Biol*. 2019;24(5):994-1007.
51. Luo Q, Xian P, Wang T, et al. Antioxidant activity of mesenchymal stem cell-derived extracellular vesicles restores hippocampal neurons following seizure damage. *Theranostics*. 2021;11(12):5986-6005.
52. Chen SY, Lin MC, Tsai JS, et al. EP4 antagonist-elicited extracellular vesicles from mesenchymal stem cells rescue cognition/learning deficiencies by restoring brain cellular functions. *Stem Cells Transl Med*. 2019;8(7):707-723.
53. Go V, Bowley BGE, Pessina MA, et al. Extracellular vesicles from mesenchymal stem cells reduce microglial-mediated neuroinflammation after cortical injury in aged rhesus monkeys. *GeroScience*. 2020;42(1):1-17.
54. Xin D, Li T, Chu X, et al. Mesenchymal stromal cell-derived extracellular vesicles modulate microglia/macrophage polarization and protect the brain against hypoxia-ischemic injury in neonatal mice by targeting delivery of miR-21a-5p. *Acta Biomater*. 2020;113:597-613.
55. Bava S, Frank LR, McQueeney T, Schweinsburg BC, Schweinsburg AD, Tapert SF. Altered white matter microstructure in adolescent substance users. *Psychiatry Res*. 2009;173(3):228-237.
56. Infante MA, Ebersson SC, Zhang Y, et al. Adolescent binge drinking is associated with accelerated decline of gray matter volume. *Cereb Cortex*. 2022;32(12):2611-2620.
57. Nguyen-Louie TT, Matt GE, Jacobus J, et al. Earlier alcohol use onset predicts poorer neuropsychological functioning in young adults. *Alcohol Clin Exp Res*. 2017;41(12):2082-2092.
58. Squeglia LM, Schweinsburg AD, Pulido C, Tapert SF. Adolescent binge drinking linked to abnormal spatial working memory brain activation: differential gender effects. *Alcohol Clin Exp Res*. 2011;35(10):1831-1841.
59. Medalla M, Chang W, Calderazzo SM, et al. Treatment with mesenchymal-derived extracellular vesicles reduces injury-related pathology in pyramidal neurons of monkey perilesional ventral pre-motor cortex. *J Neurosci*. 2020;40(17):3385-3407.
60. Go V, Sarikaya D, Zhou Y, et al. Extracellular vesicles derived from bone marrow mesenchymal stem cells enhance myelin maintenance after cortical injury in aged rhesus monkeys. *Exp Neurol*. 2021;337:113540.

61. Kaminski N, Köster C, Mouloud Y, et al. Mesenchymal stromal cell-derived extracellular vesicles reduce neuroinflammation, promote neural cell proliferation and improve oligodendrocyte maturation in neonatal hypoxic-ischemic brain injury. *Front Cell Neurosci.* 2020;14:601176.
62. Wang H, Liu Y, Li J, et al. Tail-vein injection of MSC-derived small extracellular vesicles facilitates the restoration of hippocampal neuronal morphology and function in APP/PS1 mice. *Cell Death Discov.* 2021;7(1):230.
63. Sey NYA, Gómez-A A, Madayag AC, Boettiger CA, Robinson DL. Adolescent intermittent ethanol impairs behavioral flexibility in a rat foraging task in adulthood. *Behav Brain Res.* 2019;373:112085.
64. Miller KM, Risher ML, Acheson SK, et al. Behavioral inefficiency on a risky decision-making task in adulthood after adolescent intermittent ethanol exposure in rats. *Sci Rep.* 2017;7(1):4680.
65. Macht V, Elchert N, Crews F. Adolescent alcohol exposure produces protracted cognitive-behavioral impairments in adult male and female rats. *Brain Sci.* 2020;10(11):785.

SUPPORTING INFORMATION

Additional supporting information can be found online in the Supporting Information section at the end of this article.


How to cite this article: Mellado S, Cuesta CM, Montagud S, et al. Therapeutic role of mesenchymal stem cell-derived extracellular vesicles in neuroinflammation and cognitive dysfunctions induced by binge-like ethanol treatment in adolescent mice. *CNS Neurosci Ther.* 2023;00:1-14. doi:[10.1111/cns.14326](https://doi.org/10.1111/cns.14326)

RESEARCH

Open Access



Lipidomic landscape of circulating extracellular vesicles isolated from adolescents exposed to ethanol intoxication: a sex difference study

Carla Perpiñá-Clérigues^{1,2}, Susana Mellado^{2,3}, José F. Català-Senent¹, Francesc Ibáñez³, Pilar Costa⁴, Miguel Marcos⁵, Consuelo Guerri³, Francisco García-García^{1*†} and María Pascual^{2,3*†} 

Abstract

Background Lipids represent essential components of extracellular vesicles (EVs), playing structural and regulatory functions during EV biogenesis, release, targeting, and cell uptake. Importantly, lipidic dysregulation has been linked to several disorders, including metabolic syndrome, inflammation, and neurological dysfunction. Our recent results demonstrated the involvement of plasma EV microRNAs as possible amplifiers and biomarkers of neuroinflammation and brain damage induced by ethanol intoxication during adolescence. Considering the possible role of plasma EV lipids as regulatory molecules and biomarkers, we evaluated how acute ethanol intoxication differentially affected the lipid composition of plasma EVs in male and female adolescents and explored the participation of the immune response.

Methods Plasma EVs were extracted from humans and wild-type (WT) and Toll-like receptor 4 deficient (TLR4-KO) mice. Preprocessing and exploratory analyses were conducted after the extraction of EV lipids and data acquisition by mass spectrometry. Comparisons between ethanol-intoxicated and control human female and male individuals and ethanol-treated and untreated WT and TLR4-KO female and male mice were used to analyze the differential abundance of lipids. Annotation of lipids into their corresponding classes and a lipid set enrichment analysis were carried out to evaluate biological functions.

Results We demonstrated, for the first time, that acute ethanol intoxication induced a higher enrichment of distinct plasma EV lipid species in human female adolescents than in males. We observed a higher content of the PA, LPC, unsaturated FA, and FAHFA lipid classes in females, whereas males showed enrichment in PI. These lipid classes participate in the formation, release, and uptake of EVs and the activation of the immune response. Moreover, we observed changes in EV lipid composition between ethanol-treated WT and TLR4-KO mice (e.g., enrichment of glycerophosphoinositols in ethanol-treated WT males), and the sex-based differences in lipid abundance are more notable in WT

[†]Francisco García-García and María Pascual contributed equally to this work

*Correspondence:

Francisco García-García
fgarcia@cipf.es
María Pascual
maria.pascual@uv.es

Full list of author information is available at the end of the article



mice than in TLR4-KO mice. All data and results generated have been made openly available on a web-based platform (<http://bioinfo.cipf.es/sal>).

Conclusions Our results suggest that binge ethanol drinking in human female adolescents leads to a higher content of plasma EV lipid species associated with EV biogenesis and the propagation of neuroinflammatory responses than in males. In addition, we discovered greater differences in lipid abundance between sexes in WT mice compared to TLR4-KO mice. Our findings also support the potential use of EV-enriched lipids as biomarkers of ethanol-induced neuroinflammation during adolescence.

Highlights

- Ethanol induces a differential enrichment of plasma EV lipid species in human and murine female adolescents compared to males.
- The function of these lipid species suggests that binge alcohol drinking in human female adolescents could prompt elevated EV biogenesis and a more significant immune response than in males.
- WT mice display more significant disparities in lipid abundance between sexes than TLR4-KO mice.
- The study takes a novel approach—based on bioinformatic analysis of lipidomic data—to studying the sex-based differences in the effect of alcohol.
- Plasma EV lipids represent suitable non-invasive biomarker candidates and could help to explain the mechanisms underlying the neuroinflammatory response after acute intoxication.

Keywords Lipidomics, Extracellular vesicles, Alcohol, Adolescence, Sex-based differences, Functional profiling

Plain language summary

Lipids represent essential components of extracellular vesicles (EVs), playing structural and regulatory functions during EV biogenesis, release, targeting, and cell uptake. Lipidic dysregulation has been linked to several disorders. We evaluated how acute ethanol intoxication differentially affected the lipid composition of plasma EVs in male and female adolescents and explored the participation of the immune response. Plasma EVs were extracted from humans and wild-type (WT) and Toll-like receptor 4 deficient (TLR4-KO) mice. Preprocessing and exploratory analyses were conducted after the extraction of EV lipids and data acquisition by mass spectrometry. Our analysis of differential abundance demonstrated, for the first time, that acute ethanol intoxication induced a higher enrichment of distinct plasma EV lipid species in human female adolescents than in males. We observed a higher content of the PA, LPC, unsaturated FA, and FAHFA lipid classes in females, whereas males showed enrichment in PI. These lipid classes participate in the formation, release, and uptake of EVs and the activation of the immune response. Moreover, we observed changes in EV lipid composition between ethanol-treated WT and TLR4-KO mice (e.g., enrichment of glycerophosphoinositols in ethanol-treated WT males), and the sex-based differences in lipid abundance are more notable in WT mice than in TLR4-KO mice. All data and results generated have been made openly available on a web-based platform (<http://bioinfo.cipf.es/sal>). Our findings also support the potential use of EV-enriched lipids as biomarkers of ethanol-induced neuroinflammation during adolescence.

Background

Intercellular communication is mediated by direct cell-to-cell contact and the endosomal exocytosis of secreted factors (the secretome) [1]. Extracellular vesicles (EVs), which are secreted by almost every cell type and presented in numerous body fluids, represent an important component of the cell secretome. A range of studies has demonstrated the role of EVs, which contain a wide range of DNA, RNA, lipid, and protein species, in physiological processes and pathological conditions such as inflammation, cancer, and neurodegenerative diseases

[2]. While recent research has provided extensive information concerning the protein and micro(mi)RNA content of EVs, we understand less regarding lipids, even though they play critical structural and regulatory roles during EV biogenesis, release, targeting, and cell uptake [3]. EVs often display enrichment in cholesterol, sphingomyelin, and saturated phospholipids, suggesting that EV membranes contain lipid raft-like domains [4–6]. The assembled molecular lipids and membrane-bound proteins determine the structure and function of membrane domains; therefore, a better understanding of the roles of

specific proteins and lipids that form EV membranes will provide a wealth of information regarding those mechanisms controlling EV formation, release, and subsequent function. As the specific contents of EVs from different biological fluids contain molecules tightly associated with their cell of origin [6], EVs can be considered a source of non-invasive diagnostic biomarkers for various pathological conditions [7].

As essential structural and functional molecules that impact a range of pathological conditions (including metabolic syndrome, inflammation, and neurological disorders), lipids possess huge diversity in structural and physicochemical properties, which supports their involvement in a wide range of biological functions [7]. Lipidomics has emerged as an innovative discipline that supports the discovery of novel lipid species with relevant biomedical applications [3]. Mass spectrometry-based lipidomics coupled with comprehensive computational strategies for the analysis of the large volume of data generated represents a powerful analytical tool for the identification and quantification of the lipidome of cells, tissues, or bodily fluids, which reveals subtle perturbations caused by, for example, pathological conditions, environmental stressors, or therapeutic agents [8].

Ethanol abuse during adolescence (binge alcohol drinking) can cause neuroinflammation, neurodegeneration, and cognitive dysfunction [9, 10]. Ethanol exposure activates Toll-like receptor 4 (TLR4) in glial cells to induce the release of cytokines and inflammatory mediators, which causes brain damage [11, 12]. Our previous research demonstrated that EVs play a role in the spread of ethanol-induced neuroinflammation by increasing the release of EVs enriched with inflammation-related proteins and TLR4 response-associated miRNAs [13]. Furthermore, we also discovered that adolescent females display a greater vulnerability than adolescent males to the effects of ethanol since females expressed higher levels of inflammatory molecules (e.g., cytokines,

chemokines, and EV microRNAs) than males in plasma [14, 15].

Given the critical roles of EV lipids, we employed a highly sensitive lipidomic strategy to characterize EV lipid species isolated from human and murine plasma, analyze the impact of acute ethanol intoxication on the lipid content of plasma EVs in male and female adolescents, and evaluate the differential functional roles of plasma EV lipids in the activation of immune responses.

Methods

Human subjects

Our clinical samples comprised 18 adolescents and young adults (50% females) admitted to the Emergency Department of the University Hospital of Salamanca (Spain) with moderate-to-severe acute ethanol intoxication [14–16]. Acute ethanol intoxication was defined by clinical signs and symptoms (e.g., confusion/disorientation, motor incoordination, unsteady gait, impaired reasoning, and slurred speech), blood alcohol levels (BALs) of > 1 g/L, and consumption of at least five (50 g, males) or four (40 g, females) standard drinks during the six hours before admission. Alcohol intoxication is a clinically harmful condition induced by the ingestion of a large amount of alcohol, which leads to high alcohol levels in the bloodstream [17]. Alcohol intoxication in patients is often defined as a BAL greater than 5.4–17.4 mmol/L (25–80 mg/dL or 0.025–0.080%) [18]. Of note, individuals generally failed to recall the total amount drunk or the time between the first and last intake of ethanol. Exclusion criteria were the presence of other acute (e.g., trauma or infection) or chronic illness, medication use, or suspicion/confirmation of the use of illegal drugs (apart from cannabis). Table 1 describes the clinical, epidemiological, and analytical characteristics of the individuals in this study.

Eighteen healthy controls (nine males and nine females) recruited from a body of medical and nursing

Table 1 Characteristics of study individuals displaying acute ethanol intoxication

	Males (n = 9)	Females (n = 9)
Age (years)	19.67 (0.34)	19.89 (0.50)
BALs (g/L)	2.42 (0.03)	2.12 (0.04)
Aspartate aminotransferase levels (IU/L)	30.33 (2.26)	19.11 (0.42)
Alanine aminotransferase levels (IU/L)	27.22 (3.43)	14.78 (0.49)
Alkaline phosphatase levels (IU/L)	74.22 (3.41)	59.78 (1.22)
γ -Glutamyl transpeptidase levels (IU/L)	28.22 (3.55)	12.00 (0.48)
White blood cell count/ μ L	8738.89 (274.88)	8173.33 (169.82)
Individuals who reported weekend drinking (%) [*]	6 (75.0)	8 (88.89)

Quantitative variables presented as the mean (SEM), and qualitative variables presented as absolute frequencies (percentage). IU, international units. BALs: blood alcohol levels. * A single male individual refused to answer the questionnaire regarding drinking patterns

students were also included in the study. Control individuals did not consume alcohol apart from sporadic light drinking, did not report alcohol consumption in the 72 h prior to blood extraction, and did not partake in binge drinking episodes in the three months before the study. These subjects possessed normal hematological and plasma biochemical parameters and did not report any chronic or acute illness. The study was conducted in accordance with the Declaration of Helsinki and was approved by the Ethics Committee of the University Hospital of Salamanca (November 22nd, 2012), and written informed consent was obtained from each participant. Blood samples were obtained from the patients upon admission for standard care and research purposes and used to determine BAL and for complete blood count and liver function evaluations [serum levels of aspartate aminotransferase (IU/L), alanine aminotransferase (IU/L), alkaline phosphatase (IU/L), and γ -glutamyl transpeptidase (IU/L)]. Collected serum was snap-frozen in liquid nitrogen and stored at -80°C until further use. Samples were processed and analyzed for this study only after the patients were able to provide informed consent. Figure 1A summarizes the human experimental groups.

Animals and treatment strategy

C57/BL6 wild-type (WT, $n=24$) and TLR4-knockout (TLR4-KO, $n=24$) (C57/BL6 background, kindly provided by Dr. S. Akira, Osaka, Japan) mice were used in this study. Forty-eight animals were used, with six mice per treatment group. Three to four animals were placed in each cage separated by genotype and maintained with water and a solid diet ad libitum under controlled conditions of temperature (23°C), humidity (60%), and light/dark cycles (12 h/12 h). All experimental procedures were carried out in accordance with the guidelines approved by the European Communities Council Directive (86/609/ECC) and Spanish Royal Decree 53/2013, modified by Spanish Royal Decree 1386/2018 with the approval of the Ethical Committee of Animal Experimentation of the Príncipe Felipe Research Centre (CIPE, Valencia, Spain) on June 19th, 2019 (Project identification code: 2019-08).

To model binge alcohol drinking, morning doses (9–10 a.m.) of saline or 25% (v/v) ethanol (3 g/kg) in isotonic saline were administered intraperitoneally to 30-day-old mice on two consecutive days with 2-day gaps without injections for two weeks (postnatal day [PND] 30 to PND 43), as previously described by Pascual et al. (2007) [19]. Both female and male mice displayed similar or higher BALs of ~ 320 mg/dL (peaked at 30 min post-injection) than human ethanol-intoxicated adolescents. Animals were anesthetized 24 h after the last (8th) ethanol or saline administration (PND 44), and whole blood was

collected from the hepatic portal vein. After centrifugation, the separated plasma samples were snap-frozen in liquid nitrogen and stored at -80°C until use. Figure 1A summarizes the murine experimental groups.

EV isolation from human and mouse plasma

Plasma EVs were isolated using a total exosome isolation kit (catalog number 4484450, Invitrogen, USA) following the manufacturer's instructions. 250 μL of initial plasma was used to isolate EVs, which were collected and frozen at -80°C until processing.

EVs characterization by transmission electron microscopy and nanoparticle tracking analysis

Freshly isolated EVs were fixed with 2% paraformaldehyde and prepared as previously described [13]. Preparations were examined under a transmission FEI Tecnai G2 Spirit electron microscope (FEI Europe, Eindhoven, The Netherlands) with a digital camera Morada (Olympus Soft Image Solutions GmbH, Münster, Germany). In addition, the absolute size range and concentration of EVs were analyzed using the NanoSight NS300 Malvern (NanoSight Ltd., Minton Park, UK), as previously described [13]. Figure 2 reports the characterization of EVs by electron microscopy and nanoparticle tracking analysis.

Western blot analysis

Western blotting was performed in plasma EVs for characterization purposes (Fig. 2) using a protocol described elsewhere [10]. The primary antibodies used were: anti-CD9, anti-CD63, anti-CD81, anti-calnexin (Santa Cruz Biotechnology, USA), anti-ApoB-100, and anti-ApoA-1 (Thermo Fisher Scientific, Illinois, USA). Membranes were washed, incubated with the corresponding HRP-conjugated secondary antibodies, and developed using the ECL system (ECL Plus; Thermo Fisher Scientific). Additional file 1: Figure S1 includes the whole membrane of each protein expression.

Lipid extraction

Lipids were extracted from equal amounts of plasma EVs (0.2 ml/sample) using a modified Folch extraction procedure. The last phase containing the lipids was transferred to a fresh tube, dry vacuumed with nitrogen, and stored at -80°C until further analysis. Dried samples were resuspended with isopropanol for different LC/MS acquisition methods (positive and negative-ion modes).

LC-MS/MS analysis

In fully automated Q-TOF acquisition mode, a pooled human lipid extract representing the 36 samples (four conditions \times nine replicates) was acquired by iterative

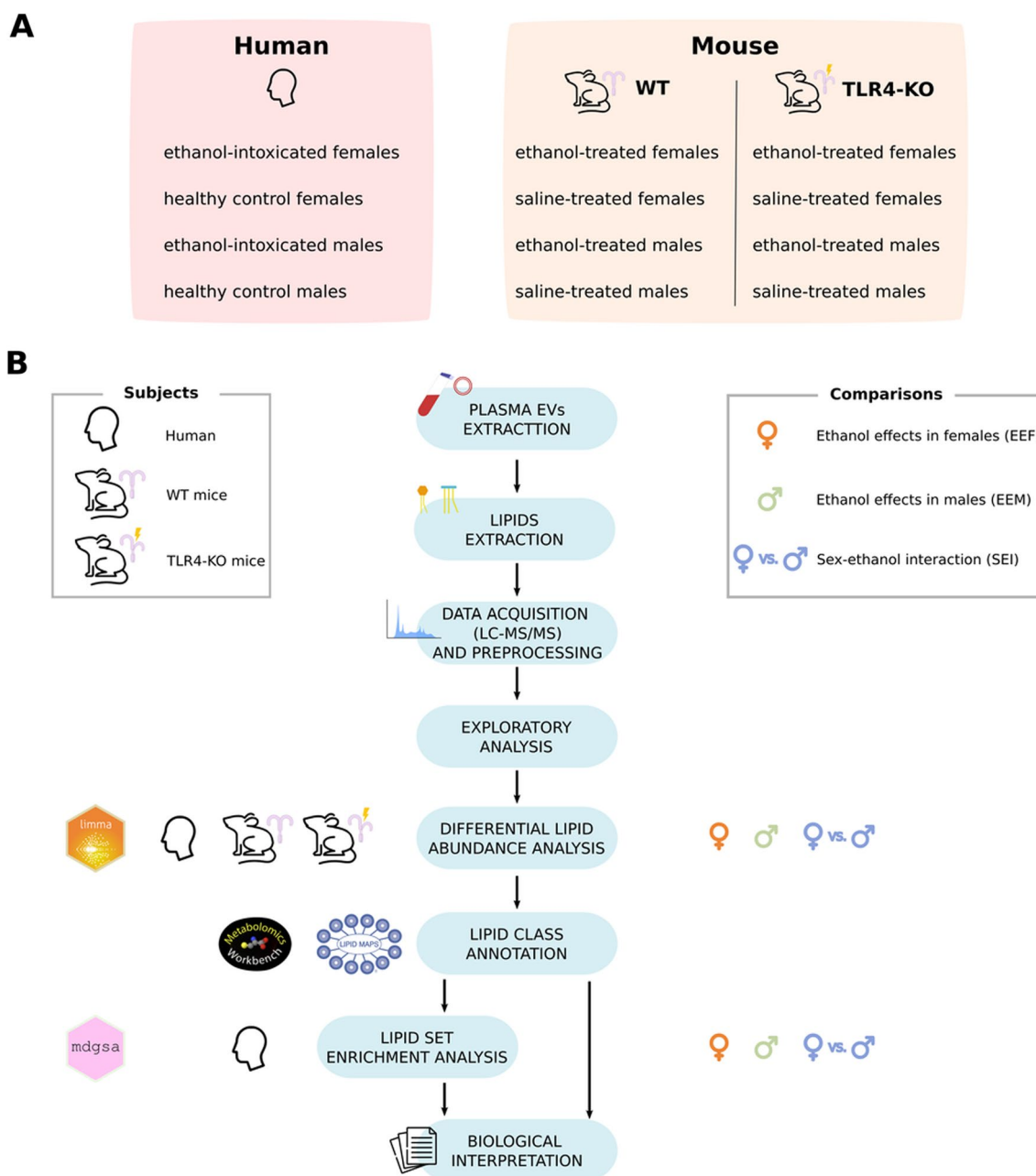


Fig. 1 Lipidomic workflow, describing the subjects analyzed and comparisons performed at each step. **A** Human and murine experimental groups. **B** After EV isolation from human and mouse blood plasma, lipids were extracted for quantification and identification by LC-MS/MS. Additional exploratory and differential lipid abundance analyses were also performed. After lipid class annotation, a class enrichment analysis was also carried out for human samples. Finally, functional profiling was applied to interpret the differential abundance analysis results

MS/MS. Detailed experimental methods for chromatography and autoMS/MS mass spectrometry were followed as described before [20, 21] with minor modifications. Briefly, sample separation was performed using an Agilent 1290 Infinity LC system coupled to the 6550 Accurate-Mass QTOF (Agilent Technologies, Santa Clara, CA, USA) with electrospray interface (Jet

Stream Technology) operating in positive-ion (3500 V) or negative-ion mode (3000 V) and high sensitivity mode. The optimal conditions for the electrospray interface were a gas temperature of 200 °C, drying gas of 12 L/min, nebulizer of 50 psi, sheath gas temperature of 300 °C, and sheath gas flow of 12 L/min. Lipids were separated on an Infinity Lab Poroshell 120 EC-C18

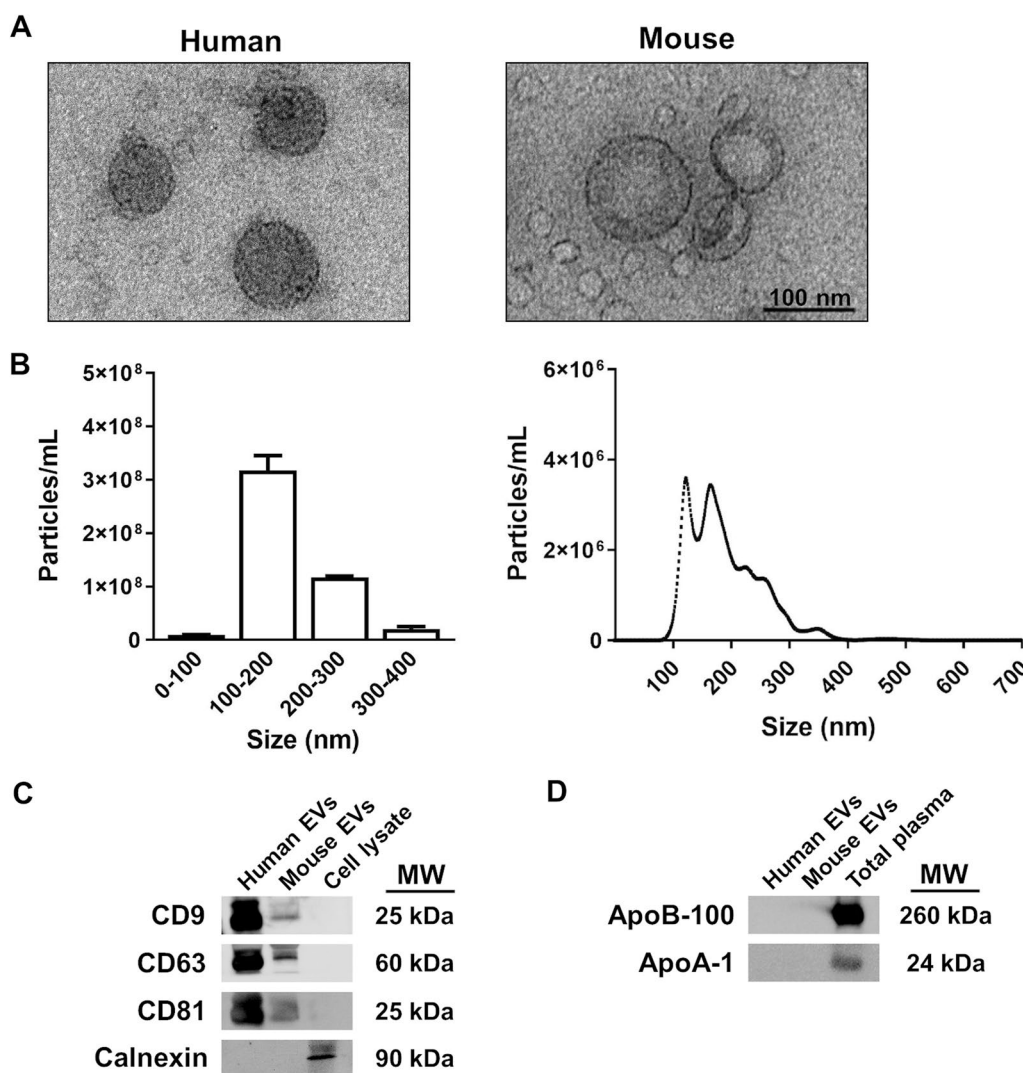


Fig. 2 Characterization of plasma EVs. **A** Electron microscopy image of human and murine EVs. **B** Measurement of human EV size distribution and concentration by nanoparticle tracking analysis. A high peak ranging between 100 and 200 nm is shown, which includes the size range of EVs. **C** Analysis of the protein expression of EV markers (CD9, CD63, and CD81) in EVs and cell lysates. Calnexin expression was used to discount cytosolic protein contamination in EV samples. Cell lysates from astroglial cells were used as a positive control for calnexin expression. **D** Expression of ApoB-100 (LDL marker) and ApoA-1 (HDL marker) to measure LDL and HDL contamination in plasma EV samples. Plasma EV samples were not contaminated by LDL and HDL particles. Total plasma was used as a positive control for ApoB-100 and ApoA-1 expression. A representative immunoblot for each protein is shown

column (3.0 × 100 mm, 2.7 μm) (Agilent, Santa Clara, CA, USA). Under optimized conditions, the mobile phase consisted of solvent A (10 mM ammonium acetate, 0.2 mM ammonium fluoride in 9:1 water/methanol) and solvent B (10 mM ammonium acetate, 0.2 mM ammonium fluoride in 2:3:5 acetonitrile/methanol/isopropanol) using the following gradient: 0 min 70% B, 1 min 70% B, 3.50 min 86% B, 10 min 86% B, 11 min 100% B, 17 min 100% B operating at 50 °C and a constant flow rate of 0.6 mL/min. The injection volume was 5 μL for positive and negative modes.

Agilent Mass Hunter Workstation Software was employed for the data acquisition. LC/MS Data Acquisition B.10.1 (Build 10.1.48) was operated in auto MS/MS, and the three most intense ions (charge states, 1–2) within a 300–1700 m/z mass range (over a threshold of 5000 counts and 0.001%) were selected for MS/MS analysis. The quadrupole was set to a “narrow” resolution (1.3 m/z), and MS/MS spectra (50–1700 m/z) were acquired until 25,000 total counts or an accumulation time limit of 333 ms. To assure the desired mass accuracy of recorded ions, a continuous internal calibration was

performed during analyses using the m/z 121.050873 and m/z 922.009798 signals for positive mode and the m/z 119.03632 and m/z 980.016375 signals for negative mode. Additionally, all-ions MS/MS [22] data were acquired on individual samples, with an MS acquisition rate of three spectra/second and four scan segments 0, 10, 20, and 40 eV.

Lipid annotator database

Five sets of five iterative MS/MS data files from pooled human cell extracts were analyzed with Lipid Annotator software 1 as the first step in the lipidomic workflow. This study used a novel software tool (Lipid Annotator) [23] with a combination of Bayesian scoring, a probability density algorithm, and non-negative least-squares fit to search a theoretical lipid library (modified LipidBlast) developed by Kind et al. [24, 25] to annotate the MS/MS spectra.

Agilent MassHunter Lipid Annotator Version 1.0 was used for all other data analyses. Default method parameters were used, except only $[M + H]^+$ and $[M + NH_4]^+$ precursors were considered for positive-ion mode analysis, and only $[M - H]^-$ and $[M + HAc - H]^-$ precursors were considered for negative-ion mode analysis. Agilent MassHunter Personal Compound Database and Library (PCDL) Manager Version B.08 SP1 was used to manage and edit the exported annotations.

Lipid identification

The lipid Personal Compound Database and Library (PCDL) databases created were used for Batch Targeted Feature Extraction in Agilent Mass Hunter Qualitative version 10.0 on the respective batches of 36 all-ions MS/MS data files. The provided “Profunder—Lipids.m” method was adapted in Mass Hunter Qualitative software with modifications previously described by Sertain et al., 2020 [21]. Data were analyzed using the Find by Formula (FbF) algorithm in MassHunter Qualitative Analysis. This approach uses a modified version of the FbF algorithm, which supports the all-ions MS/MS technique. Mass peaks in the low energy channel are first compared against the PCDL created for compounds with the same m/z values, and then a set of putative identifications is automatically compiled. For this list, the fragment ions in the MS/MS spectra from the PCDL are compared to the ions detected in the high-energy channel to confirm the presence of the correct fragments. The precursors and productions are extracted as ion chromatograms and evaluated using a coelution score. The software calculates a number that accounts for abundance, peak shape (symmetry), peak width, and retention time. The resulting compounds were reviewed in the Mass Hunter Qualitative version; features not qualified were manually

removed. Mass Hunter Qualitative results and qualified features were exported as a.cdf file.

Bioinformatic analyses

The strategy applied for this study was based on a transcriptomic analysis workflow. All bioinformatics and statistical analysis were performed using R software v.3.6.3 [26]. Figure 1B illustrates the experimental design.

Data preprocessing

Data preprocessing included filter entities, normalization of abundance lipid matrix, and exploratory analyses. Mass Hunter Qualitative results (.cdf file) were imported into Mass Profiler Professional (MPP) (Agilent Technologies) for statistical analysis, where separate experiments were created for positive and negative-ion modes. Entities were filtered based on frequency, selecting those consistently present in all replicates of at least one treatment. A percentile shift normalization algorithm (75%) was used, and datasets were baselined to the median of all samples. The median of their abundance values was calculated when duplicated lipids with different retention times were present. Data normalization was followed by exploratory analysis using cluster analysis, principal component analysis (PCA), and box and whisker plots by samples and lipids to detect abundance patterns between samples and lipids and batch effects anomalous behavior in the data. At this point, samples behaving in an anomalous manner and outliers (values that lie over $1.5 \times$ interquartile range (IQR) below the first quartile (Q1) or above the third quartile (Q3) in the data set) were excluded for presenting a robust batch effect with a critical impact on differential abundance analysis.

Differential lipid abundance

Lipid abundance levels between groups were compared using the limma R package [27]. p -values were adjusted using the Benjamini and Hochberg (BH) procedure [28], and significant lipids were considered at a BH-adjusted p -value of ≤ 0.05 .

Class enrichment analysis

Class annotation was conducted using the *RefMet* database [29] and compared with the *LIPID MAPS* database [30]. The classification is hierarchical. As an initial step in this division, lipids were divided into several principal categories (“super classes”) containing distinct main classes and sub classes of molecules, devising a standard manner of representing the chemical structures of individual lipids and their derivatives. Additional file 1: Table S1 and the legends of Figs. 5 and 6 detail all abbreviations. Annotation was followed by ordering the lipids according to the p -value and sign of the statistic obtained

in the differential lipid abundance. Similar to a Gene Set Enrichment Analysis (GSEA) method, a class enrichment analysis was carried out using Lipid Set Enrichment Analysis (LSEA) implemented in the *mdgsa* R package [31]. The *p*-values were corrected for BH, and classes with a BH-adjusted *p*-value of ≤ 0.05 were considered significant.

Comparisons

Three comparisons were performed for each group (human, WT mice, TLR4-KO mice) to analyze differential lipid abundance (Fig. 1B): (i) ethanol effects in females (EEF), which compares ethanol-intoxicated females and control females; (ii) ethanol effects in males (EEM), which compares ethanol-intoxicated males and control males; and (iii) sex–ethanol interaction (SEI), which compares EEF and EEM. Class enrichment analysis was assessed using the same three comparisons in human samples.

The statistics used to measure the differential patterns were the logarithm of fold change (LFC) to quantify the effect of differential lipid abundance analysis and the logarithm of odds ratio (LOR) to measure the enrichment of each functional class. A positive statistical sign indicates a higher mean for the variable in the first element of the comparison, whereas a negative statistical sign indicates a higher mean value for the second element. The SEI comparisons focus on finding differences between female and male comparisons. Thus, a positive statistic may indicate either upregulation in females and downregulation in males or a higher increase or a lower decrease of the variable in intoxicated female subjects. On the other hand, a negative statistic may indicate either upregulation in males and downregulation in females or a higher increase or a lower decrease of the variable in intoxicated male subjects. In this comparison, the behavior of each lipid across the groups must be assessed a posteriori, examining female and male comparisons (Additional file 1: Fig. S2).

In addition, a correlation analysis was conducted between the differential abundance results in the different comparisons, including between humans and mice. Pearson's correlation coefficient measures the relationship between these differential profiles, providing an overall picture, while the intersection of the significant lipids between comparisons provides a specific view of the results of the comparisons. The complementary nature of the approaches improves the understanding of the results of the evaluated comparisons.

Web platform

All data and results generated in the different steps of the bioinformatics analyses are available on a web platform

(<http://bioinfo.cipf.es/sal>), which is freely accessible to any user and allows the confirmation of the results described in this manuscript. The front-end was developed using the Angular Framework, the interactive graphics used in this web resource have been implemented with *plotly* [32], and the exploratory analysis cluster plot was generated with the *ggplot2* R package [33].

This easy-to-use resource is divided into seven sections: (1) a summary of analysis results; the detailed results of the (2) exploratory analysis and (3) differential abundance for each of the studies; (4) class annotation results; (5) LSEA results, where the user can interact with the web platform through graphics and tables and search for specific information related to lipid species or classes; and (6–7), which include methods, bioinformatics scripts, and Additional file 1.

Results

Sex-based differences in the lipid profiles of plasma EVs isolated from human ethanol-intoxicated adolescents

The median age of intoxicated human female and male individuals was 18.0 years (interquartile range (IQR) 18.0–21.0) and 19.0 years (IQR 19.0–20.0), respectively; these ages are considered late adolescence (ages 16–20 years) or young adulthood (ages 21–25 years) [34, 35]. The biochemical analysis of plasma during the intoxication period demonstrated median BALs of 2.10 g/L (IQR 1.80–2.20) for females and 2.40 g/L (IQR 2.25–2.73) for males. We found no evidence of other drugs of abuse in the study subjects. Overall, the BAL data exhibited a broader dispersion in females than males. Control subjects displayed a median age of 21.5 years (IQR 21.0–22.5) for females and 23.0 years (IQR 21.0–23.0) for males.

We analyzed the lipidomic profile of plasma EVs from control and ethanol-intoxicated females and males via LC–MS/MS using negative and positive-ion modes and identified 381 and 276 lipid compounds, respectively. After normalizing sample data, filtering outliers, and summarizing repeated lipids with the median, we obtained 330 and 247 lipids in negative and positive-ion modes.

We used RefMet and LIPID MAPS databases to classify all lipids identified in human subjects to characterize differences in lipid composition between ethanol-intoxicated female and male adolescents at the molecular level. Figure 3 describes the total number of super classes and main classes in the lipid profile from all human plasma EV samples (Additional file 1: Table S2 and S3 include the sub classes). Overall, the EV lipid composition displays enrichment for

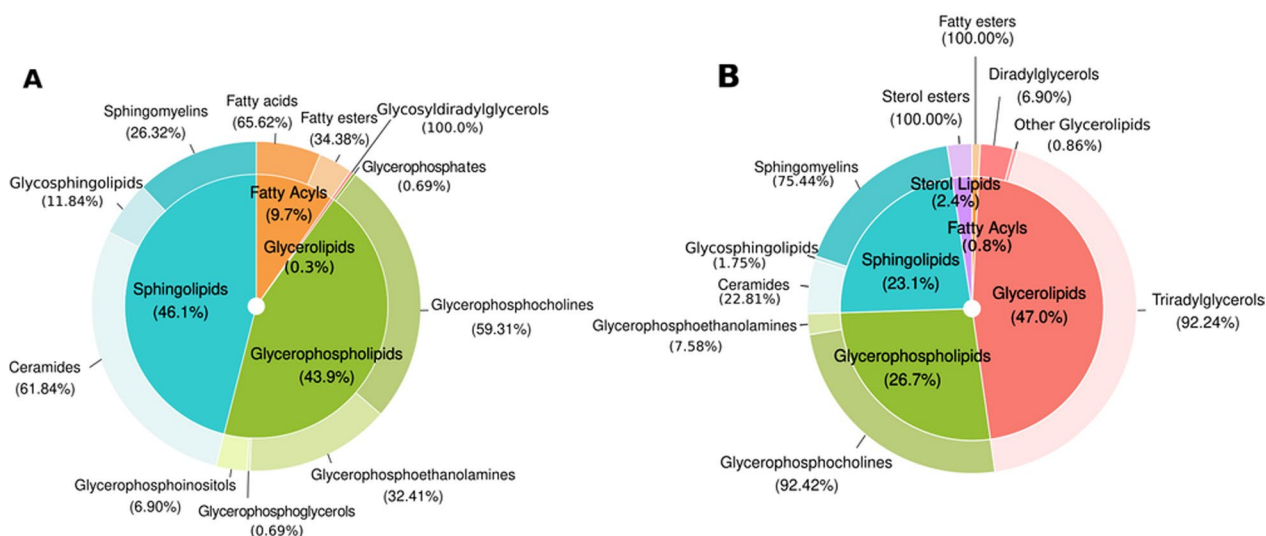


Fig. 3 Classification of total lipids in plasma EVs from human adolescents: super class (inner) and main class (outer). The super class percentages display the number of lipids that each super class represents within total lipids. The outer and inner percentages represent the total lipids in super classes and main classes obtained through the negative (A) and positive (B) ion modes

ceramides, sphingomyelins, glycerophosphocholines, and triradylglycerols, but a lower proportion of Fatty Acids and Fatty Esters.

As described in the Material and Methods section, we employed three comparisons to analyze the differential lipid abundance in human plasma EVs from distinct groups (EEF, ethanol effects in females; EEM, ethanol effects in males; SEI, sex–ethanol interaction). Table 2 describes those lipids that displayed significant changes in abundance in ethanol-intoxicated females and males compared to their respective controls. Ethanol-intoxicated females displayed a significant change in the differential abundance analysis (72 lipids), while ethanol-intoxicated males presented 33 significantly altered lipids. Furthermore, we found eight common lipids in both comparisons in both negative and positive-ion modes (Fig. 4, Additional file 1: Tables S4 and S5). The interaction of both variables (sex and treatment) revealed 24 significant lipid species, with 17 lipid species shared by EEF and SEI comparisons and five species shared

by EEM and SEI comparisons (Fig. 4, Additional file 1: Tables S4 and S5).

The relationship between EEF and EEM comparisons of LFC values for all lipids in the differential abundance analysis displayed a positive correlation in both ion modes; however, the correlation coefficient remained close to zero (negative-ion mode 0.22, positive-ion mode 0.30) (Additional file 1: Fig. S3), indicating a lack of any relationship between the variables sex and ethanol intoxication. These results provide robust evidence for sex-based differences in lipid abundance induced by ethanol intoxication.

Sex-based differences in functional lipid profiling in plasma EVs isolated from human ethanol-intoxicated adolescents

We classified significant lipid species into functional classes to analyze the lipidomes of plasma EVs in greater depth. Figure 5 reports the distribution of the classifications, which demonstrate significant

Table 2 Summary of lipids with significant abundance by both ion modes in humans

Ion mode	EEF ¹			EEM ¹			SEI ²		
	LFC > 0	LFC < 0	Total	LFC > 0	LFC < 0	Total	LFC > 0	LFC < 0	Total
Negative	26	25	51	9	4	13	9	13	22
Positive	8	13	21	10	10	20	0	2	2
Total	34	38	72	19	14	33	9	15	24

Significant lipids separated according to the sign of their log fold-change (LFC). ¹In EEF and EEM comparisons, LFC > 0 columns = differential abundance in lipids increased after ethanol exposure; LFC < 0 columns = differential abundance in lipids decreased after ethanol exposure. ²In SEI, LFC > 0 columns = differential abundance in lipids increased in females; LFC < 0 columns = Differential abundance in lipids increased in males

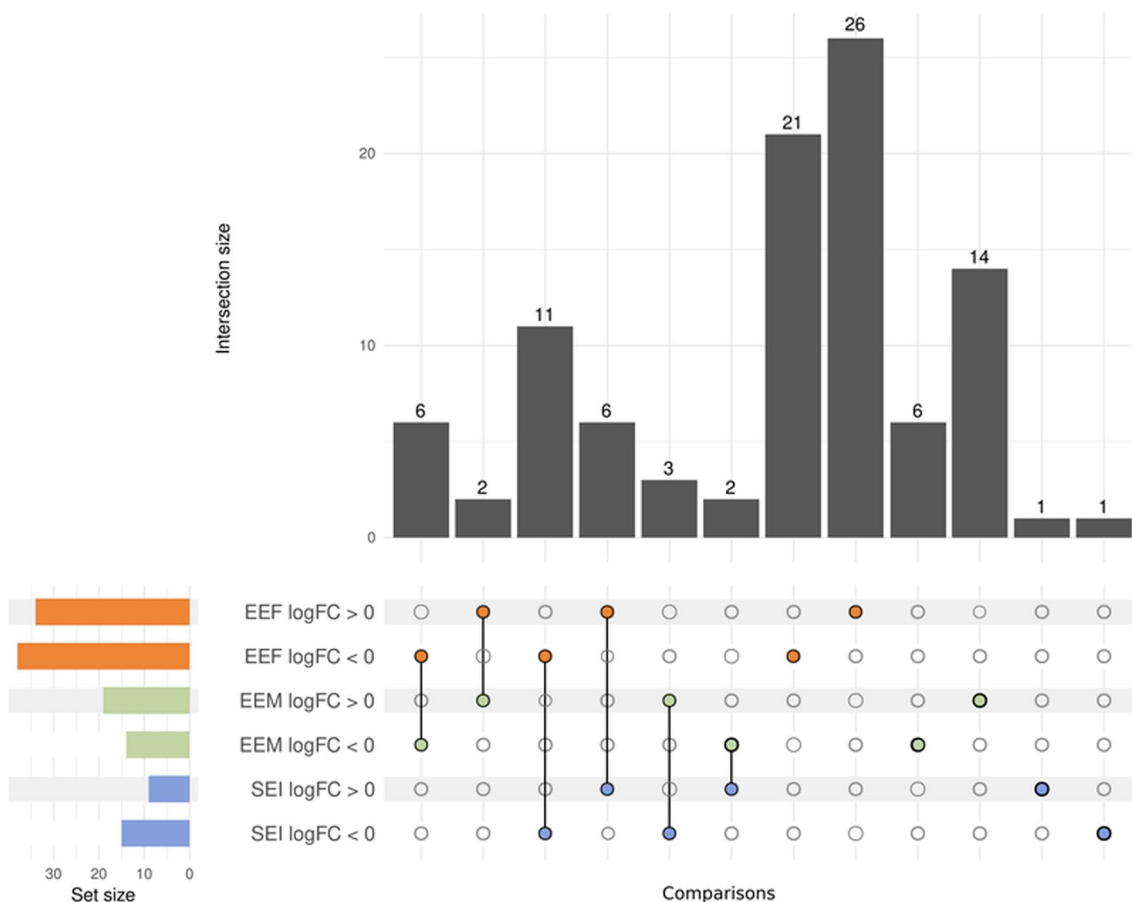


Fig. 4 Upset plot of the differential abundance analysis results from human samples. The results of each comparison are separated according to the LFC sign. Horizontal bars indicate the number of significant lipids in each comparison (a specific color for each comparison). Vertical bars indicate the lipids included in the intersection of the groups denoted with a colored dot underneath. A colored dot under a bar indicates the specificity of the genes in this group. Comparisons used: EEF (ethanol effects in females), EEM (ethanol effects in males), and SEI (sex–ethanol interaction)

differences in several of the main classes glycerophosphoinositols, glycerophosphates, glycerophosphocholine, fatty acids, and fatty esters. Sub-class analysis revealed significant enrichment in the PA, LPC, unsaturated FA, and FAHFA in plasma EVs from ethanol-intoxicated female adolescents, whereas only PI displayed upregulation in ethanol-intoxicated males;

however, we observed a much lower proportion of the sub-class cholesterol esters in ethanol-intoxicated female adolescents (Fig. 5B).

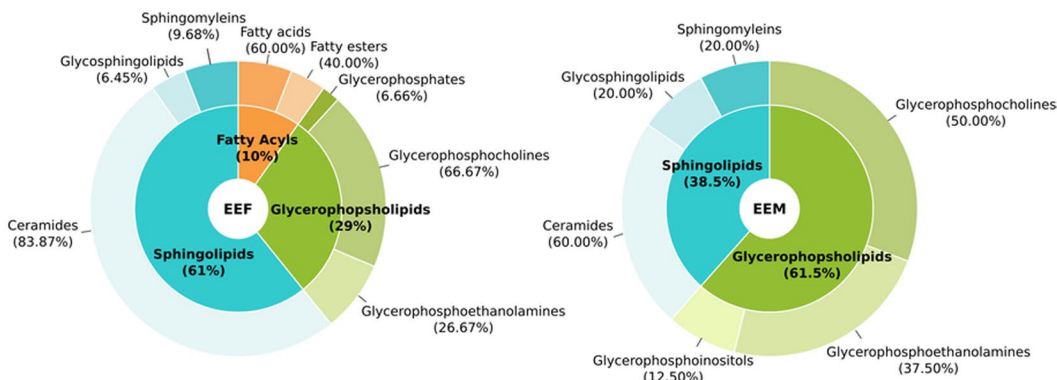
The lipid species composition of some main classes revealed the highly enriched nature of ceramides in plasma EVs isolated from ethanol-intoxicated and control females; however, we observed the downregulation

(See figure on next page.)

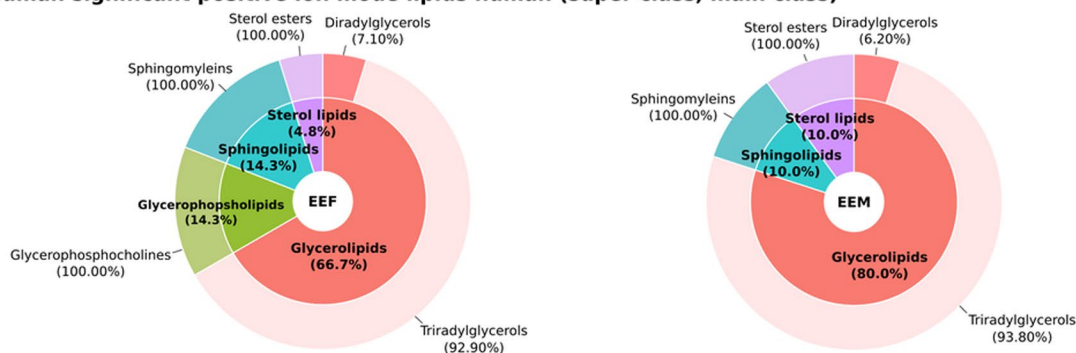
Fig. 5 Summary of lipids with significant abundance in humans by class annotation in negative and positive-ion mode. **A** The super class percentages (inner) show the number of lipids each super class represents in the total significant lipids. The main class percentages (outer) show the number of lipids each main class represents in its corresponding super class. **B** Number of significant lipids in the sub classes. The bar charts indicate the number of significant lipids in the sub classes, and the color corresponds to the main class. Comparisons used: EEF (ethanol effects in females), EEM (ethanol effects in males), and SEI (sex–ethanol interaction). Sub-class lipid abbreviations: Cer_AS, ceramide α -hydroxy fatty acid-sphingosine; Cer_NDS, ceramide non-hydroxy fatty acid-dihydrosphingosine; Cer_NP, ceramide non-hydroxy fatty acid-phytosphingosine; Cer_ADS, ceramide α -hydroxy fatty acid-dihydrosphingosine; Cer_AP, ceramide α -hydroxy fatty acid-phytosphingosine; Cer_NS, ceramide non-hydroxy fatty acid-sphingosine; HexCer_NS, glucosylCeramide/HexosylCeramidesnon-hydroxyfatty acid-sphingosine; HexCer_NDS, glucosylCeramide/HexosylCeramidesnon-hydroxyfatty acid-dihydrosphingosine; SM, sphingomyelin; FA, fatty acid; FAHFA, fatty acid ester of hydroxyl fatty acid; PA, phosphatidic acid; LPC, lyso-phosphatidylcholine; PC, phosphatidylcholine; PC-O, etherphosphatidylcholine (EtherPC); PE, phosphatidylethanolamine; PE-O, etherphosphatidylethanolamine (EtherPE); PI, phosphatidylinositol; DAG, diacylglycerol; TAG, triacylglycerol (TG); Chol. esters, cholesterol esters

A

Human significant negative ion mode lipids (super class, main class)

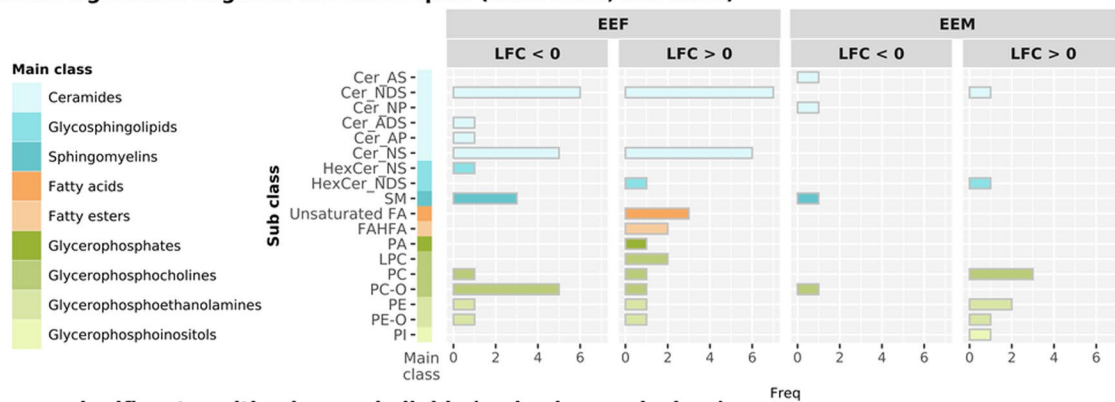


Human significant positive ion mode lipids human (super class, main class)



B

Human significant negative ion mode lipids (main class, sub class)



Human significant positive ion mode lipids (main class, sub class)

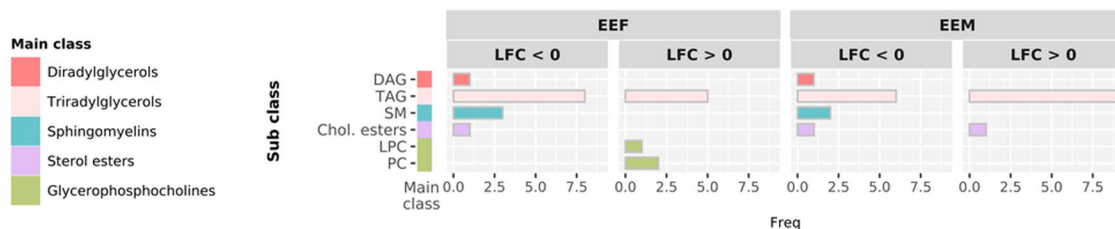


Fig. 5 (See legend on previous page.)

of some related sub classes in ethanol-intoxicated males (e.g., Cer_AS and Cer_N) and females (e.g., Cer_ADS and Cer_AP). In contrast, other main classes (e.g., diradylglycerols and sphingomyelins) displayed a similar down-regulation in abundance in ethanol-intoxicated females and males compared to their respective controls (Fig. 5B).

The LSEA results of the three human comparisons demonstrated a positive correlation with lipid classes (Fig. 6), which displayed significant differences in abundance (Fig. 5). In addition, we observed a significant enrichment of the fatty acids main class and the fatty acyls super class in the SEI comparison. In EEF, both classes possess a positive LOR value compared to EEM (negative LOR), suggesting higher lipid abundance in ethanol-intoxicated females than males (Fig. 6). We also observed a significantly higher enrichment of the glycerophosphoethanolamines and PC main classes and the Cer_NS sub-class in ethanol-intoxicated males than in control males; however, we also observed a significantly lower enrichment of Cer_ADS in ethanol-intoxicated males. Finally, we encountered a significantly higher enrichment of the LPC sub-class in ethanol-intoxicated females than in control females (Fig. 6).

Sex-based differences in lipid profiles of plasma EVs isolated from ethanol-treated adolescent mice

We next evaluated potential sex-based differences in ethanol-induced alterations in EV lipid composition and the involvement of the TLR4-mediated immune response in these effects. We analyzed lipid species in control and adolescent ethanol-treated WT and TLR4-KO mice. The lipidomic analyses demonstrated 326 and 289 lipid compounds for the negative and positive-ion modes; we obtained 291 and 264 lipid species in negative and positive-ion modes for further differential analysis after data processing.

We employed RefMet and LIPID MAPS databases to characterize the differences in lipid composition between ethanol-treated female and male adolescent mice at the molecular level. The quantitative data analysis obtained for all lipid species in plasma EVs revealed similar percentages of lipid classes (super and main classes, Additional file 1: Tables S6 and S7 include the sub classes) in the negative and positive-ion modes between adolescent mice (Fig. 7A and B) and human individuals (Fig. 3). Figure 7C and D displays the 182 negative and 124 positive common lipids in human and murine samples. Figure 7A

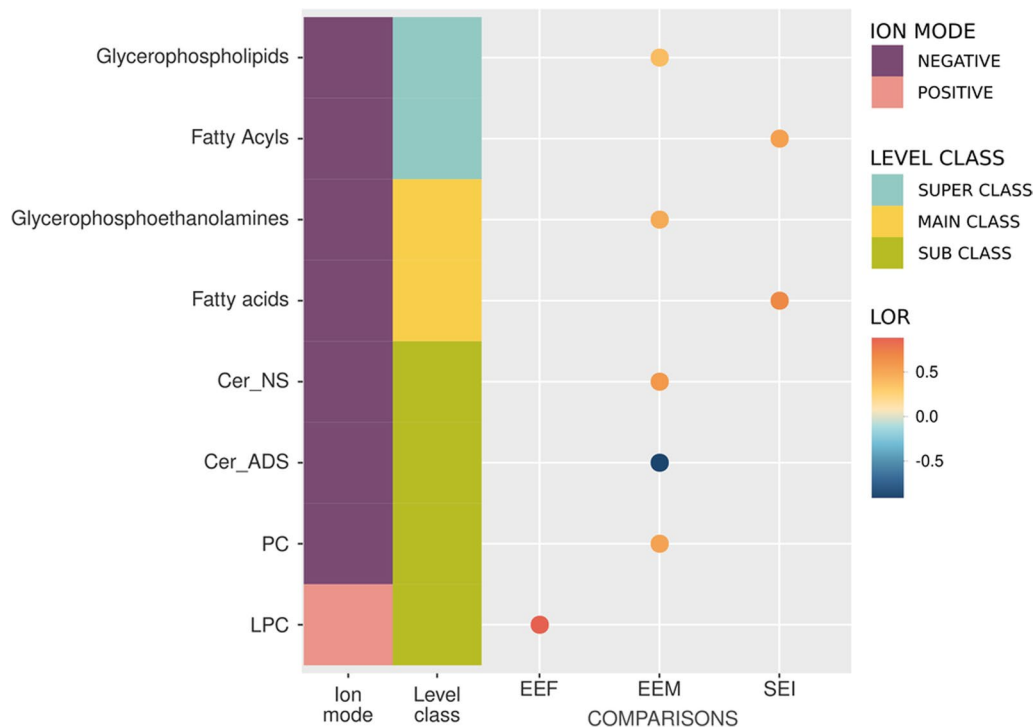


Fig. 6 Enriched significant lipid classes in humans by LSEA. The color of the dots represents the sign and magnitude of the change (LOR). Comparisons used: EEF (ethanol effects in females), EEM (ethanol effects in males), and SEI (sex-ethanol interaction). Sub-class lipid abbreviations: Cer_NS, ceramide non-hydroxy fatty acid-sphingosine; Cer_ADS, ceramide α -hydroxy fatty acid-dihydrosphingosine; PC, phosphatidylcholine; LPC, lyso-phosphatidylcholine

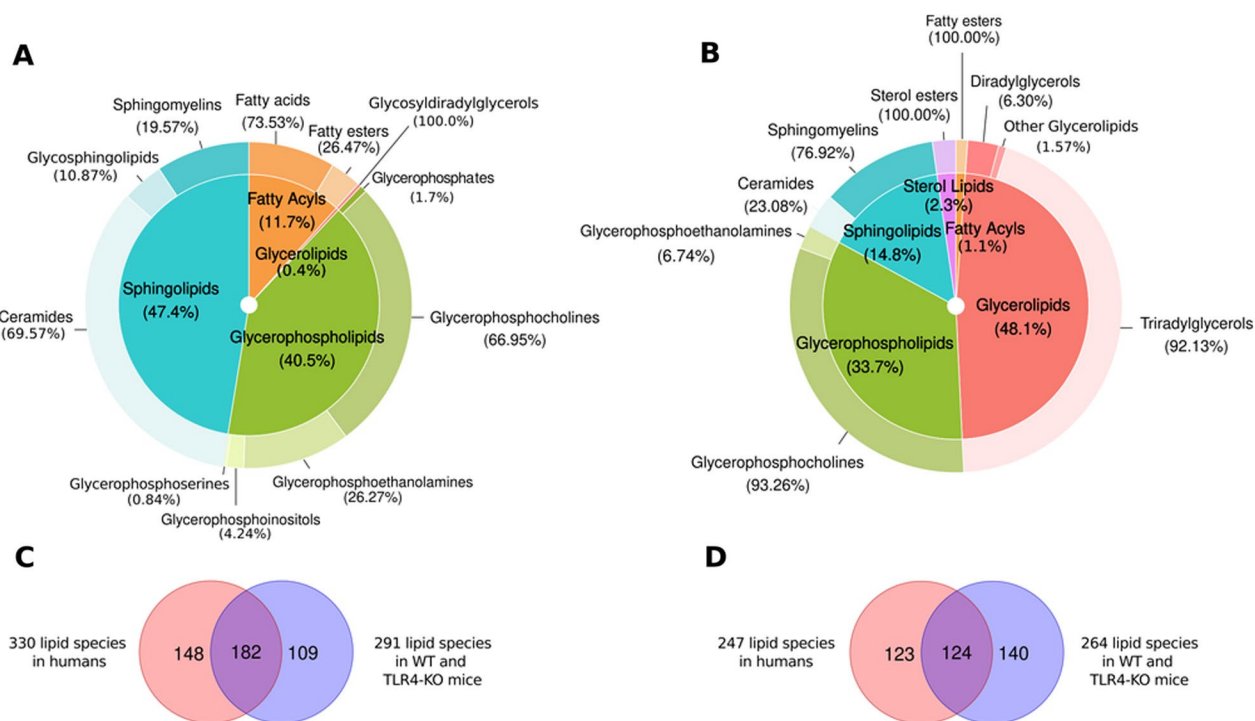


Fig. 7 Classification of total lipids in plasma EVs from WT and TLR4-KO adolescent mice: super class (inner) and main class (outer). The super class percentages show the number of lipids that each super class represents in the total lipids. The outer and inner percentages represent the total lipids in the super class and main class obtained through the negative (A) and positive (B) ion modes. The Venn diagram intersection represents the common lipid species between human and murine samples in negative (C) and positive (D) ion modes

and B demonstrates that EV lipid composition in mice displays an enrichment for ceramides, sphingomyelins, glycerophosphocholines, and triradylglycerols with a lower proportion of fatty acids and fatty esters; however, we observed differences in some main and sub classes between human and murine samples (e.g., glycerophosphoglycerol enrichment only occurred in humans, while glycerophosphoserine enrichment only occurred in mice).

Tables 3 and 4 show that ethanol-treated female and male WT mice presented significant changes in 12 and 47 lipid species, respectively; meanwhile, ethanol-treated TLR4-KO female and male mice presented significant

changes in 66 and 58 lipid species, respectively. Figure 8 demonstrates that female and male mice treated with ethanol shared one lipid in WT mice and ten lipids in TLR4-KO mice. Female WT and TLR4-KO mice displayed only one significantly differential lipid species in common (Fig. 8); meanwhile, male WT and TLR4-KO mice presented nine common lipid species, although three exhibited different lipid patterns (Fig. 8, Additional file 1: Table S8–S11). In addition, we observed a different lipid abundance pattern between EEF WT and EEM WT (low correlation coefficient) in both lipid ion modes (Additional file 1: Fig. S3); in contrast, we encountered a

Table 3 Summary of lipids with significant abundance using both ion modes in WT mice

Mouse	Ion mode	EEF ¹			EEM ¹			SEI ²		
		LFC > 0	LFC < 0	Total	LFC > 0	LFC < 0	Total	LFC > 0	LFC < 0	Total
WT	Negative	5	2	7	14	7	21	10	5	15
	Positive	3	2	5	12	14	26	2	3	5
Total		8	4	12	26	21	47	12	8	20

Significant lipids separated according to the sign of their log fold-change (LFC). ¹In EEF and EEM comparisons, LFC > 0 columns = differential abundance in lipids increased after ethanol treatment; LFC < 0 columns = differential abundance in lipids decreased after ethanol treatment. ²In SEI, LFC > 0 columns = differential abundance in lipids increased in females; LFC < 0 columns = Differential abundance in lipids increased in males

Table 4 Summary of lipids with significant abundance using both ion modes in TLR4-KO mice

Mouse	Ion mode	EEF ¹			EEM ¹			SEI ²		
		LFC > 0	LFC < 0	Total	LFC > 0	LFC < 0	Total	LFC > 0	LFC < 0	Total
TLR4-KO	Negative	25	38	63	15	7	22	1	0	1
	Positive	2	1	3	22	14	36	2	0	2
Total		27	39	66	37	21	58	3	0	3

Significant lipids separated according to the sign of their log fold-change (LFC). ¹In EEF and EEM comparisons, LFC > 0 columns = differential abundance in lipids increased after ethanol treatment; LFC < 0 columns = differential abundance in lipids decreased after ethanol treatment. ²In SEI, LFC > 0 columns = differential abundance in lipids increased in females; LFC < 0 columns = differential abundance in lipids increased in males

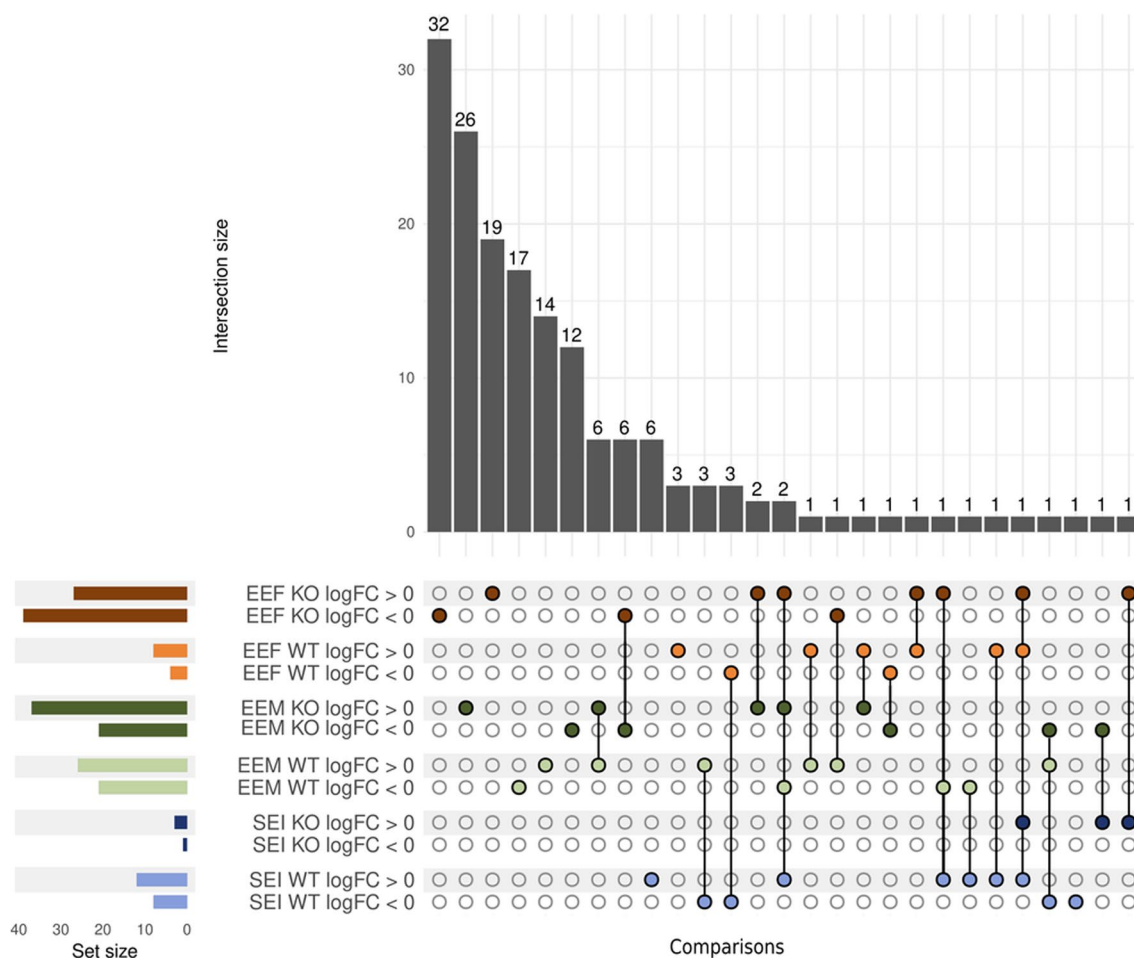


Fig. 8 Upset plot of the differential abundance analysis results in WT and TLR4-KO mouse samples. The results of each comparison are separated according to the LFC sign. Horizontal bars indicate the number of significant lipids in each comparison (a specific color for each comparison). Vertical bars indicate the lipids included in the intersection of the groups denoted with a colored dot underneath. A colored dot under a bar indicates the specificity of the genes in this group. Comparisons used in WT and TLR4-KO mice: EEF (ethanol effects in females), EEM (ethanol effects in males), and SEI (sex-ethanol interaction)

similar lipid profile for EEF TLR4-KO and EEM TLR4-KO (high and significant correlation coefficient). We also observed a significant positive correlation between human females and WT females (EEF, EEF WT) in lipids (negative-ion mode) (Additional file 1: Fig. S3).

Sex-based differences in functional lipid profiling in plasma EVs isolated from ethanol-treated adolescent mice

Figure 9 demonstrates the downregulation of most of the main classes of lipids (e.g., glycerolipids and other

glycerolipids) in ethanol-treated female WT mice but the upregulation of ceramides, glycosphingolipids and sphingomyelins. Interestingly, we observed the downregulation of Diradylglycerols in ethanol-treated WT males and the upregulation of glycerophosphoinositols and sphingomyelins. When studying alterations in main class lipids in plasma EVs isolated from TLR4-KO mice, we observed differences in the fatty esters and fatty acids main classes in ethanol-treated female TLR4-KO mice and other glycerolipids in ethanol-treated male TLR4-KO mice (Fig. 10). The fatty acyls super class only possessing significance in TLR4-KO mice and the sterol lipids super class only possessing significance in WT animals represent the main differences between ethanol-treated WT and TLR4-KO mice (Figs. 9A, 10A). At the main class level, we observed several significant differences in TLR4-KO and WT mice; however, the results differ in terms of abundance (Figs. 9B, 10B). The other glycerolipids main class became downregulated in ethanol-treated WT females and ethanol-treated TLR4-KO males. In contrast, we only observed the diradylglycerols and glycerophosphoinositols main classes in control and ethanol-treated WT male mice, respectively. When we compared humans and WT mice, only the glycerophosphoinositols main class displayed a common pattern (Figs. 5 and 9).

Web platform

The web platform (<http://bioinfo.cipf.es/sal>) contains detailed information regarding the complementary computational approaches involved in this study. This resource includes statistical indicators of each performed analysis for each organism, which users can explore to identify their profiles of interest. This open resource hopes to contribute to data sharing between researchers, elaborating innovative studies, and discovering new findings.

Discussion

Our recent results demonstrated the involvement of EVs as possible amplifiers and biomarkers of ethanol-induced neuroinflammation. We found an increased level of vulnerability of human female adolescents compared to males to the effects of ethanol, with ethanol-intoxicated females exhibiting fewer anti-inflammatory microRNAs in plasma EVs than males [15]. In addition to microRNAs, EVs also contain various lipid species that could represent regulatory molecules and/or biomarkers. A lipidomic strategy combined with computational data analysis demonstrated,

for the first time, that acute ethanol intoxication induces a higher enrichment of EV lipid species (e.g., PA, LPC, unsaturated FA, and FAHFA) in human female adolescents than in males. These lipid species are associated in the formation, release, and uptake of EVs (e.g., PA and LPC) [3, 36–40] and the activation of the immune response (e.g., PA, LPC, and unsaturated FA) [3, 41]. Although we also observed changes in EV lipid composition between ethanol-treated WT and TLR4-KO mice, the sex-based differences in the lipid abundance were more notable in WT mice than in TLR4-KO mice.

Ethanol treatment increases EV release from astroglial cells and enriches their content of inflammation-related proteins and miRNAs, which may be associated with the amplification of neuroinflammation [13]. Lipid metabolism participates in EV formation and secretion [3, 42], and a recent study revealed that ethanol alters lipid metabolism by increasing cholesterol uptake through mitochondria-associated endoplasmic reticulum membrane activity, cholesterol esterification, and sphingomyelinase activity in microglia [43]. EVs often display enrichment in cholesterol and sphingomyelin [4], with the conversion of sphingomyelin into ceramide by sphingomyelinases closely linked to EV biogenesis [44]. Accordingly, we observed a decrease in the sphingomyelin sub-class and enrichment of HexCer_NDS and some Cer in plasma EVs from human ethanol-intoxicated females and males, which could be associated with EV formation. In addition, the HexCer_NDS (glycosphingolipids) main class also displayed greater abundance in female ethanol-treated WT mice. This main class participates in EV release, and ceramide may also play a cell-dependent role in EV formation in PC3 cells [45]. Furthermore, ceramides are also essential for the secretion of EVs by facilitating or inducing membrane curvature [3, 36]. Interestingly, ethanol-intoxicated human females (but not males) displayed enrichment in PA and LPC species in plasma EVs. Various reports have described the involvement of the PA sub-class in the formation, secretion, and fusion of EVs and protein–lipid interactions [3, 36–39]. Subra et al. (2010) [40] reported that LPC participated in the fusion of EVs with the endosome-limiting membrane, allowing the release of any EV content into the cytosol.

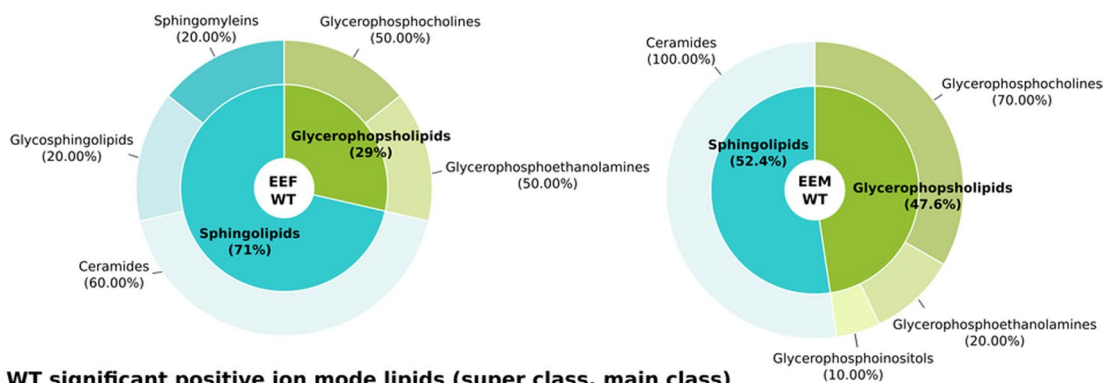
EVs directly transport lipids from parental cells to recipient cells, which may activate different signaling pathways. For instance, the fatty acids main class or LPC

(See figure on next page.)

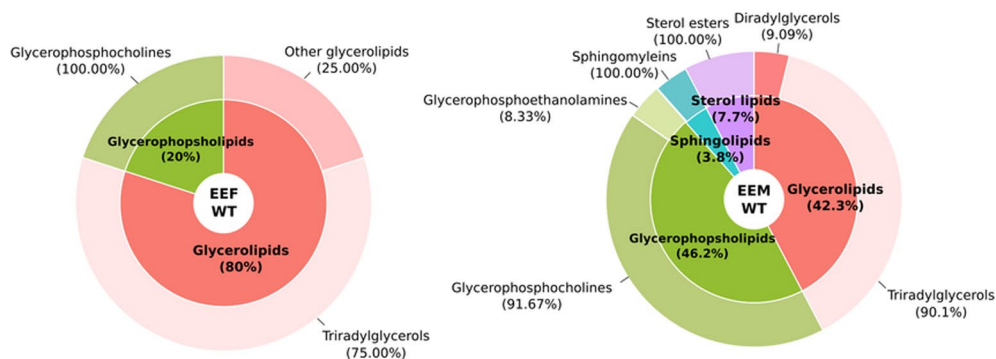
Fig. 9 Summary of lipids with significant abundance in WT mice using different class annotations. **A** The super class percentages (inner) show the number of lipids each super class represents in the total significant lipids. The main class percentages (outer) show the number of lipids each main class represents in its corresponding super class. **B** Number of significant lipids in the main classes. The bar charts indicate the number of significant lipids in the main classes. Comparisons used in WT mice: EEF (ethanol effects in females), EEM (ethanol effects in males), and SEI (sex–ethanol interaction)

A

Mice WT Significant negative ion mode lipids (super class, main class)

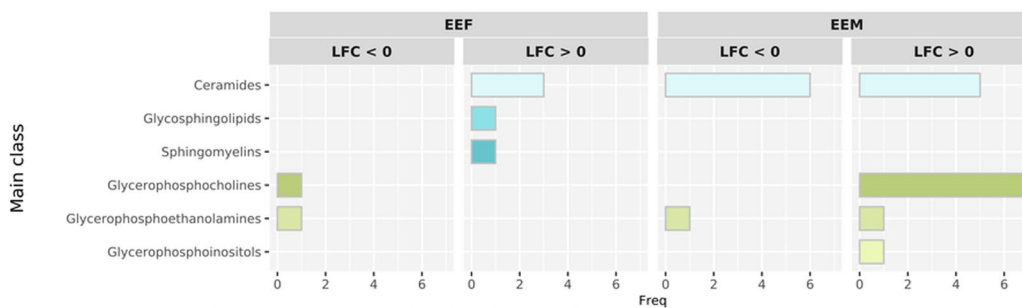


Mice WT significant positive ion mode lipids (super class, main class)



B

Mice WT significant negative ion mode lipids (main class)



Mice WT significant positive ion mode lipids (main class)

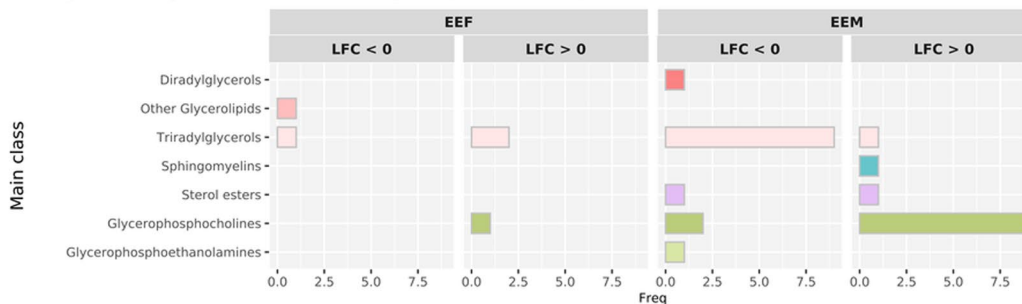


Fig. 9 (See legend on previous page.)

(glycerophosphocholines main class) can induce inflammatory processes or immune responses [3, 46], such as NF κ B activation through the TLR4 signaling pathway [41]. In addition, LPS- or phagocytosis-mediated glycerophosphoinositol (e.g., PI) production may participate in the inflammatory responses of macrophages and other immune cells [47]. Herein, we observed that ethanol-intoxicated human female adolescents displayed a significant enrichment of LPC, unsaturated FA, and FAHFA in plasma EVs; however, ethanol-intoxicated males only displayed higher amounts of PI. Overall, these findings suggest that binge drinking in human female adolescents induces a more robust immune response than in males. The enrichment of the noted lipid classes could be used as a biomarker for ethanol-induced neuroinflammation during adolescence since EV lipids already represent robust non-invasive diagnostic and prognostic biomarkers for several brain diseases [48, 49].

TLRs are embedded in cellular membranes, and the posttranslational lipid modification of these membranes regulates the dynamic associations of these receptors with membrane lipid raft microdomains [50]. Our previous studies demonstrated that ethanol induces TLR4 recruitment into lipid rafts upon activation, which leads to the release of cytokines and inflammatory mediators and causes brain damage [11, 12, 51]; furthermore, we revealed that TLR4-deficient mice failed to display an ethanol-induced inflammatory immune response [12]. Recent studies reported that changes in cellular lipid organization might promote or inhibit TLR recruitment into lipid rafts, which can trigger or attenuate receptor-dependent signaling processes [50]. Our results provide evidence for the enrichment of chol. esters and PI in plasma EVs isolated from ethanol-treated WT male mice, whereas no changes occurred in ethanol-treated TLR4-deficient male mice. Cholesterol is required for the biogenesis, release, and stability of EVs and their uptake by target cells [52] and participates in lipid raft formation [5]; meanwhile, as previously mentioned, PI (Glycerophosphoinositols main class) mediates immune responses [47]. In addition, ethanol-treated TLR4-deficient females presented lower levels of unsaturated FA and FAHFA in plasma EVs than in the other comparisons reported in this study. Considering the relation of Fatty acids to inflammation [3, 41], these results suggest that changes in EV lipid composition in ethanol-treated

TLR4-deficient mice could inhibit inflammatory immune responses.

We previously demonstrated that both human and WT mouse females displayed a greater level of vulnerability to the effects of ethanol since females expressed higher levels of plasma proinflammatory molecules than males [14, 15]; moreover, a study by Grange et al. revealed similar EV miRNA expression profiles between humans and rat/mouse models [53]. Our current data demonstrate that the Glycerophosphoinositols main class, associated with the immune response [47], becomes upregulated in human and WT mouse males in response to alcohol. The HexCer_NDS (Glycosphingolipids) main class, which has been associated with EV release [45], also increased in human ethanol-intoxicated human adolescents and female ethanol-treated WT mice; however, if we look deeper into the results pertaining to the mouse model of this study, we observe a more notable disparity in lipid abundance between sexes in WT mice than in TLR4-KO mice.

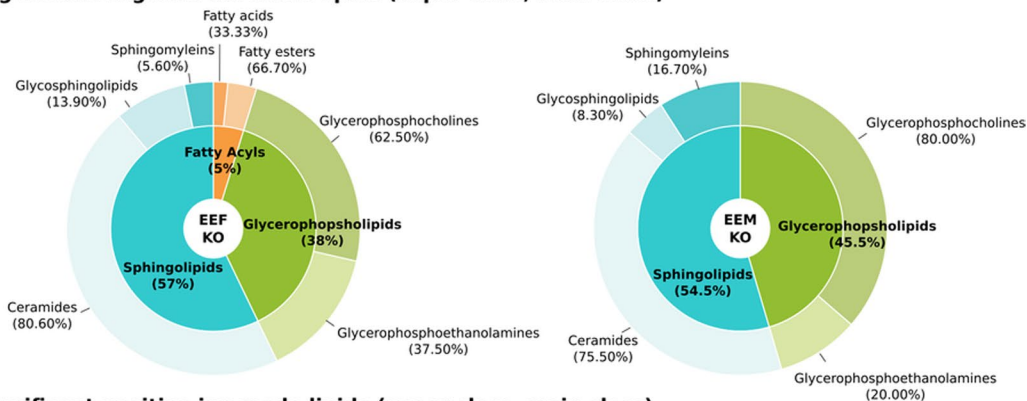
We are aware of certain limitations related to the present study. The use of lipidomic technology in this study represented a challenge concerning the design and application of the bioinformatics strategy to address: (1) the lack of standardization of lipid nomenclature and its integration into the analysis software, (2) the extension of analysis methodologies from genomics and transcriptomics to lipidomics, and (3) the generation of functional annotation [3]. Although there is some evidence that the EVs used in this study might indeed be exosomes, it is actually challenging to distinguish exosomes from microvesicles, as both can be of similar size and express similar markers. Furthermore, we cannot rule out the existence of unknown, significant differences between the human subjects (cases vs. controls) that may limit the comparison regarding lipid composition between groups. Despite these factors, our present study takes a novel approach to the study of sex-based differences in the effect of alcohol based on the bioinformatic analysis of lipidomic data. Our findings will also improve the understanding of the effects of binge drinking by including a gender perspective. All data, results, and programming scripts have been included in open resources (web platform and Zenodo repository) for sharing with the scientific community.

(See figure on next page.)

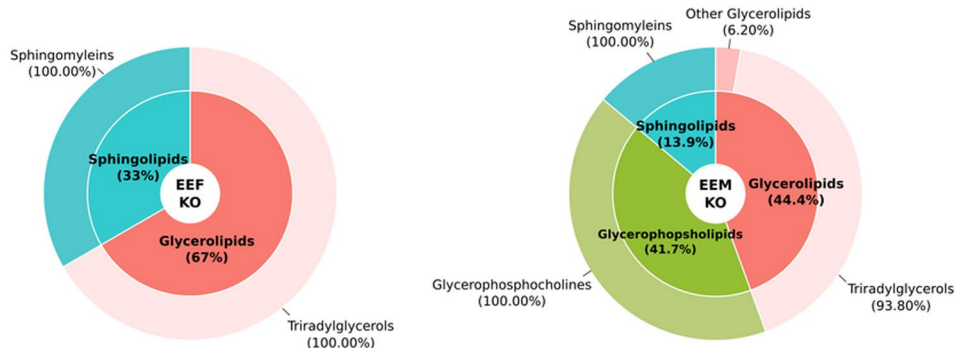
Fig. 10 Summary of lipids with significant abundance in TLR4-KO mice using different class annotations. **A** The super class percentages (inner) show the number of lipids each super class represents in the total significant lipids. The main class percentages (outer) show the number of lipids each main class represents in its corresponding super class. **B** Number of significant lipids in the main class. The bar charts indicate the number of significant lipids in the main class. Comparisons used in TLR4-KO mice: EEF (ethanol effects in females), EEM (ethanol effects in males), and SEI (sex-ethanol interaction)

A

Mice KO Significant negative ion mode lipids (super class, main class)

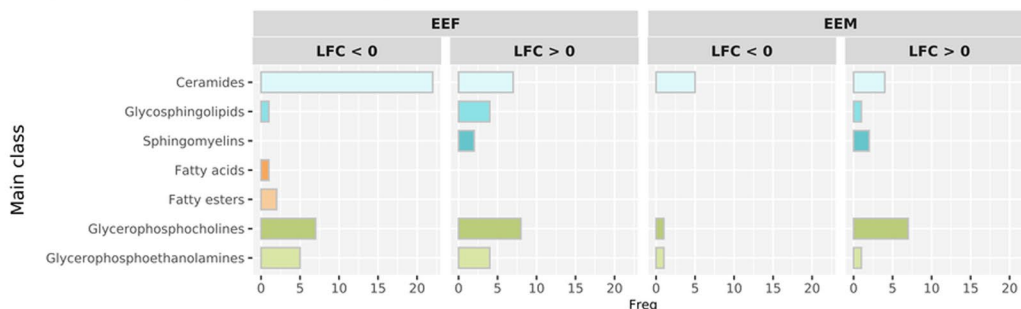


Mice KO significant positive ion mode lipids (super class, main class)



B

Mice KO significant negative ion mode lipids (main class)



Mice KO significant positive ion mode lipids (main class)

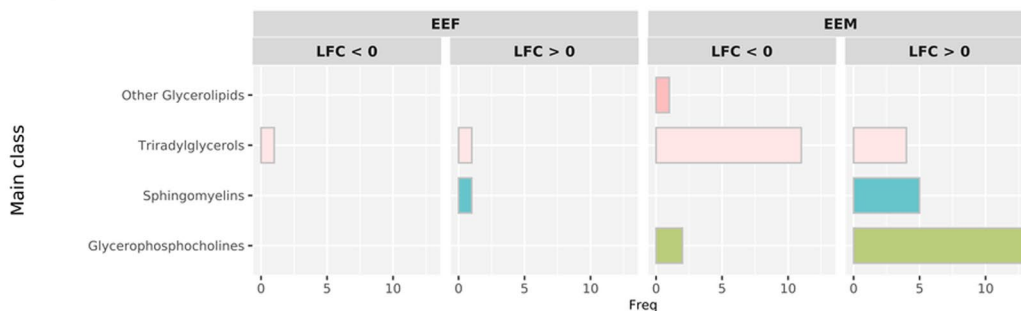


Fig. 10 (See legend on previous page.)

Perspectives and significance

Our results support the existence of differences between female and male adolescents in EV lipidomic profiles induced in response to binge alcohol drinking. Given the vulnerability of women to alcohol's effects, this work suggests the use of sex-specific differences in EV lipids to help understand the mechanisms involved during alcohol consumption and provide suitable candidates for non-invasive sex-specific biomarkers (e.g., TG 16:0_18:1_20:3 and Cer_NDS d39:1 in human females and males). The present study takes a novel approach to assess the sex differences in the effect of ethanol on the lipidomic profile through a comprehensive bioinformatic strategy.

Conclusions

For the first time, these results indicate that ethanol induces a differential enrichment of EV lipid species in human female adolescents compared to males. These lipid species participate in EV formation, release, and uptake, inflammatory immune responses, and TLR4 activation, which suggests that binge alcohol drinking in human female adolescents could be associated with higher levels of EV biogenesis and inflammatory processes than in males. Furthermore, we observed more notable differences in lipid abundance between sexes in WT mice than in TLR4-KO mice. Finally, our sex-based differential analysis of EV-resident lipids could provide suitable candidates for non-invasive biomarkers and help to explain the mechanisms underlying the neuroinflammatory response after acute intoxication. Thus, our approach provides a breakthrough for studies related to one of society's most serious problems, ethanol abuse in the form of binge drinking.

Supplementary Information

The online version contains supplementary material available at <https://doi.org/10.1186/s13293-023-00502-1>.

Additional file 1. Additional material associated to methods and results.

Acknowledgements

The authors thank the Príncipe Felipe Research Center (CIPF) for providing access to the cluster, which is co-funded by European Regional Development Funds (FEDER) in Valencian Community 2014–2020. The authors also thank the Genomics and Proteomics Unit at the University of Alicante, the Electron Microscopy Service at the Príncipe Felipe Research Centre, Irene Soler-Sáez for designing Additional file 1: Figure S2, and Stuart P. Atkinson for reviewing the manuscript.

Author contributions

CPC analyzed the data; MP and FGG designed and supervised the bioinformatics analysis; PC and MM obtained human plasma samples; SM and FI isolated EVs from human and mouse plasma; CPC and JFC designed and implemented the web tool; CPC, MP, and FGG wrote the manuscript; CPC designed the graphical abstract; CPC, MP, and FGG helped in the interpretation of the

results; CPC, JFC, MM, CG, MP, and FGG writing—review and editing; MP and FGG conceived the work. All authors read and approved the final manuscript.

Funding

This work has been supported by grants from the Spanish Ministry of Health-PNSD (2019-I039), GVA (CIAICO/2021/203), the Carlos III Institute and FEDER funds (RTA-Network, RD16/0017/0004), the Primary Addiction Care Research Network (RD21/0009/0005), FEDER Funds, GVA and the Instituto de Salud Carlos III (ISCIII) through the project PI20/00743, co-funded by the European Union and the Junta de Castilla y León (GRS 2388/A/21), PID2021-124430OA-I00 funded by MCIN/AEI/10.13039/501100011033/FEDER, UE ("A way to make Europe"), and partially funded by the Institute of Health Carlos III (project IMPaCT-Data, exp. IMP/00019), co-funded by the European Union, European Regional Development Fund (ERDF, "A way to make Europe"). C. Perpiñá-Clérigues was supported by a predoctoral fellowship from the Generalitat Valenciana (ACIF/2021/338).

Availability of data and materials

The datasets generated and analyzed during the current study and programming scripts are available in the Zenodo repository, <http://doi.org/10.5281/zenodo.6581012>, and in a web platform: <http://bioinfo.cipf.es/sal>.

Declarations

Ethics approval and consent to participate

Human plasma samples were used in accordance with the Declaration of Helsinki and were approved by the Ethics Committee of the University Hospital of Salamanca (November 22nd, 2012), and written informed consent was obtained from each participant. All animal procedures were carried out in accordance with the guidelines approved by European Communities Council Directive (86/609/ECC) and Spanish Royal Decree 1201/2005 with the approval of the Ethical Committee of Animal Experimentation of the Príncipe Felipe Research Centre (Valencia, Spain) on June 19th, 2019 (Project identification code: 2019-08).

Consent for publication

Not applicable.

Competing interests

The authors declare that they have no competing interests.

Author details

¹Bioinformatics and Biostatistics Unit, Príncipe Felipe Research Center, C/ Eduardo Primo Yúfera, 3, 46012 Valencia, Spain. ²Department of Physiology, School of Medicine and Dentistry, University of Valencia, Avda. Blasco Ibáñez, 15, 46010 Valencia, Spain. ³Department of Molecular and Cellular Pathology of Alcohol, Príncipe Felipe Research Center, 46012 Valencia, Spain. ⁴Emergency Department, University Hospital of Salamanca-IBSAL, University of Salamanca, 37007 Salamanca, Spain. ⁵Department of Internal Medicine, University Hospital of Salamanca, Institute of Biomedical Research of Salamanca (IBSAL), University of Salamanca, 37007 Salamanca, Spain.

Received: 24 October 2022 Accepted: 3 April 2023

Published online: 21 April 2023

References

- Meinken J, Walker G, Cooper CR, Min XJ. MetazSecKB: the human and animal secretome and subcellular proteome knowledgebase. Database. 2015;2015:bav077.
- Frühbeis C, Fröhlich D, Kuo WP, Krämer-Albers E-M. Extracellular vesicles as mediators of neuron-glia communication. Front Cell Neurosci. 2013;7:182.
- Donoso-Quezada J, Ayala-Mar S, González-Valdez J. The role of lipids in exosome biology and intercellular communication: function, analytics and applications. Traffic. 2021;22:204–20.
- Trajkovic K, Hsu C, Chiantia S, Rajendran L, Wenzel D, Wieland F, et al. Ceramide triggers budding of exosome vesicles into multivesicular endosomes. Science. 2008;319:1244–7.

5. de Gassart A, Géminard C, Février B, Raposo G, Vidal M. Lipid raft-associated protein sorting in exosomes. *Blood*. 2003;102:4336–44.
6. Skotland T, Hessvik NP, Sandvig K, Llorente A. Exosomal lipid composition and the role of ether lipids and phosphoinositides in exosome biology. *J Lipid Res*. 2019;60:9–18.
7. Hu T, Zhang J-L. Mass-spectrometry-based lipidomics. *J Sep Sci*. 2018;41:351–72.
8. Wenk MR. The emerging field of lipidomics. *Nat Rev Drug Discov*. 2005;4:594–610.
9. Montesinos J, Pascual M, Pla A, Maldonado C, Rodríguez-Arias M, Miñarro J, et al. TLR4 elimination prevents synaptic and myelin alterations and long-term cognitive dysfunctions in adolescent mice with intermittent ethanol treatment. *Brain Behav Immun*. 2015;45:233–44.
10. Montesinos J, Pascual M, Rodríguez-Arias M, Miñarro J, Guerri C. Involvement of TLR4 in the long-term epigenetic changes, rewarding and anxiety effects induced by intermittent ethanol treatment in adolescence. *Brain Behav Immun*. 2016;53:159–71.
11. Blanco AM, Vallés SL, Pascual M, Guerri C. Involvement of TLR4/Type I IL-1 receptor signaling in the induction of inflammatory mediators and cell death induced by ethanol in cultured astrocytes. *J Immunol*. 2005;175:6893–9.
12. Fernández-Lizarbe S, Pascual M, Guerri C. Critical role of TLR4 response in the activation of microglia induced by ethanol. *J Immunol*. 2009;183:4733–44.
13. Ibáñez F, Montesinos J, Ureña-Peralta JR, Guerri C, Pascual M. TLR4 participates in the transmission of ethanol-induced neuroinflammation via astrocyte-derived extracellular vesicles. *J Neuroinflammation*. 2019;16:136.
14. Pascual M, Montesinos J, Marcos M, Torres J-L, Costa-Alba P, García-García F, et al. Gender differences in the inflammatory cytokine and chemokine profiles induced by binge ethanol drinking in adolescence: ethanol and gender differences. *Addict Biol*. 2017;22:1829–41.
15. Ibáñez F, Ureña-Peralta JR, Costa-Alba P, Torres J-L, Laso F-J, Marcos M, et al. Circulating MicroRNAs in extracellular vesicles as potential biomarkers of alcohol-induced neuroinflammation in adolescence: gender differences. *Int J Mol Sci*. 2020;21:6730.
16. López-Moreno JA, Marcos M, Calleja-Conde J, Echeverry-Alzate V, Bühler KM, Costa-Alba P, et al. Histone deacetylase gene expression following binge alcohol consumption in rats and humans. *Alcohol Clin Exp Res*. 2015;39:1939–50.
17. Vonghia L, Leggio L, Ferrulli A, Bertini M, Gasbarrini G, Addolorato G. Acute alcohol intoxication. *Eur J Intern Med*. 2008;19:561–7.
18. Canfield DV, Dubowski KM, Cowan M, Harding PM. Alcohol limits and public safety. *Forensic Sci Rev*. 2014;26:9–22.
19. Pascual M, Blanco AM, Cauli O, Miñarro J, Guerri C. Intermittent ethanol exposure induces inflammatory brain damage and causes long-term behavioural alterations in adolescent rats. *Eur J Neurosci*. 2007;25:541–50.
20. Sartain M, Salcedo J, Murali A, Li X, Stow S, Koelmel J. Improving Coverage of the Plasma Lipidome Using Iterative MS/MS Data Acquisition Combined with Lipid Annotator Software and 6546 LC/Q-TOF. *Agilent Application Note* 2019, 5994–0775en; 2019.
21. Sartain M, Van de Bittner G, Stow S. Lipid Profiling Workflow Demonstrates Disrupted Lipogenesis Induced with Drug Treatment in Leukemia Cells. Combined with Lipid Annotator and 6546 LC/Q-TOF. *Agilent Application Note* 2020, 5994–1356en; 2020.
22. Agilent Technologies. All Ions MS/MS: Targeted Screening and Quantitation Using Agilent TOF and Q-TOF LC/MS Systems. *Agilent Technologies Technical Overview* 2013, 5991–2465en.
23. Koelmel JP, Li X, Stow SM, Sartain MJ, Murali A, Kemperman R, et al. Lipid annotator: towards accurate annotation in non-targeted liquid chromatography high-resolution tandem mass spectrometry (LC-HRMS/MS) lipidomics using a rapid and user-friendly software. *Metabolites*. 2020;10:101.
24. Kind T, Liu K-H, Lee DY, DeFelice B, Meissen JK, Fiehn O. LipidBlast in silico tandem mass spectrometry database for lipid identification. *Nat Methods*. 2013;10:755–8.
25. Tsugawa H, Caija T, Kind T, Ma Y, Higgins B, Ikeda K, et al. MS-DIAL: data-independent MS/MS deconvolution for comprehensive metabolome analysis. *Nat Methods*. 2015;12:523–6.
26. R Core Team. R: A Language and Environment for Statistical Computing. Vienna, Austria: R Foundation for Statistical Computing. <https://www.R-project.org>
27. Ritchie ME, Phipson B, Wu D, Hu Y, Law CW, Shi W, et al. limma powers differential expression analyses for RNA-sequencing and microarray studies. *Nucleic Acids Res*. 2015;43:e47–e47.
28. Benjamini Y, Hochberg Y. Controlling the False Discovery Rate: A Practical and Powerful Approach to Multiple Testing. *J R Stat Soc Ser B Methodol*. 1995;57:289–300.
29. Fahy E, Subramaniam S. RefMet: a reference nomenclature for metabolomics. *Nat Methods*. 2020;17:1173–4.
30. Sud M, Fahy E, Cotter D, Brown A, Dennis EA, Glass CK, et al. LMSD: LIPID MAPS structure database. *Nucleic Acids Res*. 2007;35:D527–32.
31. Montaner D, Dopazo J. Multidimensional gene set analysis of genomic data. *PLoS ONE*. 2010;5: e10348.
32. Sievert C. Interactive Web-Based Data Visualization with R, plotly, and shiny. Chapman and Hall/CRC; 2020. <https://plotly-r.com>.
33. Wickham H. ggplot2: Elegant Graphics for Data Analysis. Springer-Verlag New York; 2016. <https://ggplot2.tidyverse.org>.
34. Brown SA, McGue M, Maggs J, Schulenberg J, Hingson R, Swartzwelder S, et al. A developmental perspective on alcohol and youths 16 to 20 years of age. *Pediatrics*. 2008;121(Supplement_4):S290–310.
35. Masten AS, Faden VB, Zucker RA, Spear LP. A developmental perspective on underage alcohol use. *Alcohol Res Health J Natl Inst Alcohol Abuse Alcohol*. 2009;32:3–15.
36. Wang G, Wang Y, Liu N, Liu M. The role of exosome lipids in central nervous system diseases. *Rev Neurosci*. 2020;31:743–56.
37. Hirsova P, Ibrahim SH, Krishnan A, Verma VK, Bronk SF, Werneburg NW, et al. Lipid-induced signaling causes release of inflammatory extracellular vesicles from hepatocytes. *Gastroenterology*. 2016;150:956–67.
38. Kooijman EE, Chupin V, Fuller NL, Kozlov MM, de Kruijff B, Burger KNJ, et al. Spontaneous curvature of phosphatidic acid and lysophosphatidic acid. *Biochemistry*. 2005;44:2097–102.
39. Subra C, Laulagnier K, Perret B, Record M. Exosome lipidomics unravels lipid sorting at the level of multivesicular bodies. *Biochimie*. 2007;89:205–12.
40. Subra C, Grand D, Laulagnier K, Stella A, Lambeau G, Paillasse M, et al. Exosomes account for vesicle-mediated transcellular transport of activatable phospholipases and prostaglandins. *J Lipid Res*. 2010;51:2105–20.
41. Calder PC. Fatty acids and inflammation: the cutting edge between food and pharma. *Eur J Pharmacol*. 2011;668:550–8.
42. Record M, Silvente-Poirot S, Poirot M, Wakelam MJO. Extracellular vesicles: lipids as key components of their biogenesis and functions. *J Lipid Res*. 2018;59:1316–24.
43. Ibáñez F, Montesinos J, Area-Gomez E, Guerri C, Pascual M. Ethanol induces extracellular vesicle secretion by altering lipid metabolism through the mitochondria-associated ER membranes and sphingomyelinases. *Int J Mol Sci*. 2021;22:8438.
44. Shamseddine AA, Airola MV, Hannun YA. Roles and regulation of neutral sphingomyelinase-2 in cellular and pathological processes. *Adv Biol Regul*. 2015;57:24–41.
45. Phuyal S, Skotland T, Hessvik NP, Simolin H, Øverbye A, Brech A, et al. The ether lipid precursor hexadecylglycerol stimulates the release and changes the composition of exosomes derived from PC-3 cells. *J Biol Chem*. 2015;290:4225–37.
46. Law S-H, Chan M-L, Marathe GK, Parveen F, Chen C-H, Ke L-Y. An updated review of lysophosphatidylcholine metabolism in human diseases. *Int J Mol Sci*. 2019;20:1149.
47. Patrusi L, Mariggio S, Corda D, Baldari CT. The glycerophosphoinositols: from lipid metabolites to modulators of t-cell signaling. *Front Immunol*. 2013;4:213.
48. Skotland T, Sandvig K, Llorente A. Lipids in exosomes: current knowledge and the way forward. *Prog Lipid Res*. 2017;66:30–41.
49. Lazar I, Clement E, Attane C, Muller C, Nieto L. A new role for extracellular vesicles: how small vesicles can feed tumors' big appetite. *J Lipid Res*. 2018;59:1793–804.
50. Köberlin MS, Heinz LX, Superti-Furga G. Functional crosstalk between membrane lipids and TLR biology. *Curr Opin Cell Biol*. 2016;39:28–36.

51. Blanco AM, Perez-Arago A, Fernandez-Lizarbe S, Guerri C. Ethanol mimics ligand-mediated activation and endocytosis of IL-1R/TLR4 receptors via *lipid rafts* caveolae in astroglial cells. *J Neurochem*. 2008;106:625–39.
52. Pfrieger FW, Vitale N. Thematic review series: exosomes and microvesicles: lipids as key components of their biogenesis and functions, cholesterol and the journey of extracellular vesicles. *J Lipid Res*. 2018;59:2255–61.
53. Grange C, Tritta S, Tapparo M, Cedrino M, Tetta C, Camussi G, et al. Stem cell-derived extracellular vesicles inhibit and revert fibrosis progression in a mouse model of diabetic nephropathy. *Sci Rep*. 2019;9:4468.

Publisher's Note

Springer Nature remains neutral with regard to jurisdictional claims in published maps and institutional affiliations.

Ready to submit your research? Choose BMC and benefit from:

- fast, convenient online submission
- thorough peer review by experienced researchers in your field
- rapid publication on acceptance
- support for research data, including large and complex data types
- gold Open Access which fosters wider collaboration and increased citations
- maximum visibility for your research: over 100M website views per year

At BMC, research is always in progress.

Learn more biomedcentral.com/submissions

